Reflectance of Zooplankton and its Detectability by Fishes

by

Robert Ho Gochian

B.Sc., Simon Fraser University, 2017

Thesis Submitted in Partial Fulfillment of the
Requirements for the Degree of
Master of Science

in the
Department of Biological Sciences
Faculty of Science

SIMON FRASER UNIVERSITY
Spring 2022

Declaration of Committee

Name:	**Robert Gochian**
Degree:	**Master of Science**
Thesis title:	**Reflectance of Zooplankton and its Detectability by Fishes**
Committee:	**Chair:** **Harald Hutter** Professor, Biological Sciences
	Iñigo Novales Flamarique Supervisor Professor, Biological Sciences
	Leah Bendell Committee Member Professor, Biological Sciences
	Gerhard Gries Committee Member Professor, Biological Sciences
	Vicki Marlatt Examiner Associate Professor, Biological Sciences

Abstract

Few studies have investigated reflected ultraviolet and polarized light cues from zooplankton and how these optical properties affect their contrast to zooplanktivorous fishes. An optical setup was used to measure the reflectance of three zooplankton species. In conjunction with measures of photoreceptor absorptance and environmental irradiance, the contrast of zooplankton was estimated with respect to the visual systems of rainbow trout (*Oncorhynchus mykiss*) and zebrafish (*Danio rerio*). Antagonistic cone mechanisms involving either ultraviolet-sensitive cones or short-wavelength sensitive cones with middle-wavelength sensitive cones and long-wavelength sensitive cones resulted in the greatest contrast of *Daphnia* to both fishes. When modeling involved polarized irradiance, there were no significant differences in contrast as a function of polarization, likely due to the small sample size of zooplankton analyzed. Overall, the results corroborate previous findings suggesting that shorter wavelength cone mechanisms play crucial roles in enhancing zooplankton detection.

Keywords: zooplankton reflectance; visual contrast; diffuse light; polarized light; rainbow trout; zebrafish

To my exemplary teachers, past and present, whose kind encouragement and steadfast guidance had opened my “lenses” to the bewitchment of biology.

Acknowledgements

I would like to thank my senior supervisor, Professor Inigo Novales Flamarique, and my supervisory committee, Professors Leah Bendell and Gerhard Gries. I would also like to thank my 4D Labs collaborators, Professor Gary Leach and Dmitry Star, as well as Moira Galbraith from Fisheries and Oceans Canada. Lastly, I would like to thank my former colleague in the lab, Reo Zukoshi.

Table of Contents

List of Tables

List of Figures

List of Acronyms

DAS	Downwelling and sidewelling antisun irradiances
DS	Downwelling and sidewelling sun irradiances
HF	Horizontal factor
L cone	Long-wavelength sensitive cone
M cone	Middle-wavelength sensitive cone
nm	nanometre
RT	Rainbow trout
S cone	Short-wavelength sensitive cone
UV	Ultraviolet
UV cone	Ultraviolet-sensitive cone
Z	Zebrafish

Glossary

Light	As an oscillating wave, light has electric and magnetic fields, which are orthogonal to each other.
Linearly polarized light	Light that has its electric field fixed in a certain orientation as it oscillates, usually expressed as either horizontally and perpendicularly polarized light, or P-polarized and S-polarized light, respectively.
Opsin	A protein that is covalently bound to a vitamin-A derivative, forming a visual pigment.
P-polarized light	A state of linearly polarized light wherein the wave is oscillating in a plane parallel to the plane of incidence.
Plane of incidence	The plane through which an incident beam travels as it meets a reflective surface and is reflected by it. The plane of incidence is perpendicular to the plane of the reflective surface.
Zooplanktivorous	Relating to an organism that mostly consumes zooplankton
S-polarized light	A state of linearly polarized light wherein the wave is oscillating in a plane perpendicular to the plane of incidence.
Unpolarized light	Light wherein the degree of linear polarization is random, usually originating from a natural light source, i.e., the sun.

Chapter 1.

Introduction

Several planktivorous fishes—such as zebrafish (*Danio rerio*), the young life stages of salmonid fishes (genus *Oncorhynchus*), and yellow perch (*Perca flavescens*)—use ultraviolet (UV) vision to improve the contrast of zooplankton prey (Browman et al., 1994; Cronin & Bok, 2016; Loew et al., 1993; Novales Flamarique, 2013, 2016). Rainbow trout (*Oncorhynchus mykiss*) and zebrafish are believed to perceive the reflected ultraviolet light from *Daphnia*, a cladoceran zooplankton, and from some other microorganisms, such as *Paramecia*, thus making them more visible (Novales Flamarique, 2013, 2016; Yoshimatsu et al., 2020; Zimmermann et al., 2018). However, precise measurements of zooplankton reflectance in the UV and visible ranges—wavelength (λ) range: 320-760 nm—are not available although these are key variables to model the visual contrasts of zooplankton (Novales Flamarique, 2013).

In addition to contrast that arises from diffuse light reflections, polarized light reflections may be used by polarization-sensitive predators to detect zooplankton (Johnsen et al., 2011; Novales Flamarique 2019; Novales Flamarique & Browman, 2001; Shashar et al., 1998; Zukoshi et al., 2018). Among vertebrates, the only proven polarization visual system is that described for the northern anchovy (*Engraulis mordax*) where two axially dichroic cone photoreceptor types form an orthogonal polarization detection system in the ventro-temporal retina (Novales Flamarique, 2017). This arrangement of orthogonally-oriented dichroic photoreceptors resembles that found in many insects and stomatopod crustaceans (Labhart, 2016), endowing the northern anchovy with the ability to double its mean sighting distance of zooplankton in comparison with foraging under unpolarized conditions (Novales Flamarique 2019). It is believed that polarized light reflections from zooplankton exoskeletons may play a role in enhancing their contrast to anchovies (Fineran & Nicol, 1978; Kondrashev et al., 2012; Kondrashev et al., 2016; Novales Flamarique 2017, 2019). Measurements of polarized light reflections from zooplankton are lacking; however, such that visual contrast estimates under different polarized light backgrounds have not been carried out.

Although both UV and polarization cues likely play important roles in the ability to detect zooplankton by small planktivorous fishes, a lack of information regarding the reflectance properties of zooplankton has impeded accurate modeling of the enhanced visual contrasts imparted to fish visual systems by these attributes of light.

1.1. Physical attributes of light

1.1.1. Light has three physical attributes: wavelength, intensity, and polarization

Light consists of photons, each an electromagnetic wave comprising of electric and magnetic field components that oscillate perpendicular to each other and to the direction of propagation (Hecht & Zajac, 1979; Schurcliff, 1962). Animal visual systems can only detect the electric field of light (Fein and Szuts, 1982). Light has three physical attributes that animals can sense to assess their surroundings: wavelength (colour), intensity (number of photons), and polarization (the plane of electric field oscillation) (Fein and Szuts, 1982).

The vertebrate visual spectrum spans wavelengths from 320 nm to 700 nm (Jacobs, 1992; Levine, 1985). This range is limited by lens transmission in the ultraviolet wavelengths (Douglas & Jeffery, 2014) and by visual pigment absorption in the long wavelengths (Kennedy & Milkman, 1956). Perception of ultraviolet light (i.e., wavelengths below 400 nm) is primarily a property of non-mammalian visual systems, which often have lenses transmitting down to 320 nm and retinal cones that absorb maximally in the ultraviolet range (Cronin & Bok, 2016; Douglas & Jeffery, 2014; Kennedy & Milkman, 1956).

The polarization of light refers to the plane of oscillation of the main electric field from the ensemble of photons that comprise the light source (Hecht and Zajac, 1979; Schurcliff 1962). Light that has all its photons with electric fields oscillating in the same plane is said to be linearly polarized in that plane. Diffuse (unpolarized) light from the sun is rendered partially or fully polarized in various ways including reflection from surfaces and dielectric materials, scattering by small particles in the atmosphere (Rayleigh scattering), and passage through optically active (e.g., dichroic or birefringent) materials (Hecht and Zajac, 1979).

1.1.2. Reflection and transmittance at an interface

Light at an interface will generate reflected (Figure 1) and transmitted components (Figure 2) according to Snell's Law (Equation 1):

$$\frac{\sin\theta_i}{\sin\theta_t} = \frac{n_2}{n_1} \quad (1)$$

Snell's Law describes the relationship between the angle that a beam of incidence light makes (θ_i) as it hits the interface (in relation to the normal of the interface) and the angle of the wave's transmittance (θ_t) through the interface into the second medium (Lvovsky, 2013), wherein n_1 is the refractive index of the first medium and n_2 is that of the second (Figure 1.2).

1.1.3. Polarization of reflected and transmitted components at an interface

When polarized light is reflected at an interface, both reflected light and transmitted rays will be partially polarized (Lvovsky, 2013). The polarization of light is described in terms of two components: the P-polarization, when the electric field component is parallel to the plane of incidence (Figure 1.3), and the S-polarization, when the component of the electric field is perpendicular to the plane of incidence (Figure 1.4). The P-polarized and S-polarized components of reflected and transmitted light can be calculated using Fresnel's equations (Hecht & Zajac, 1979; Schurcliff, 1962).

1.2. The vertebrate retina

1.2.1. Photoreceptors and visual pigments

The vertebrate retina is a multilayered neuronal structure containing two types of specialized neurons (rod and cone photoreceptors) that absorb light to begin the process of phototransduction. Rods mediate vision in dim-light environments whereas cones operate in colour in bright-light conditions and are responsible for colour vision. There are two main morphological types of cone photoreceptors: single and double cones. Whereas single cones have circular cross sections, double cones consist of two single cones apposed together sharing a double membrane partition and exhibit elliptical cross

section (Cheung et al., 2013). Single and double cones form repeating arrangements across the retina termed mosaics (Frau et al., 2020).

Rod and cone photoreceptors contain visual pigments in their outer segments. Each visual pigment is composed of a protein (opsin) that is covalently bound to a chromophore—a vitamin A derivative (Hárosi, 1994, Cronin & Bok, 2016; Cronin & Johnsen, 2016). The outer segment of a photoreceptor is a modified cilium consisting of lipid bilayers called lamellae.

Visual pigments have light absorbances that depend on both the opsin type and the chromophore, the latter being based on vitamin A1 or vitamin A2 (Cronin & Johnsen, 2016; Ebrey & Koutalos, 2001; Yokoyama, 2000). For a given opsin, an association with a vitamin A2 chromophore will produce a visual pigment with longer wavelength of maximum absorbances than an association with a vitamin A1 chromophore (Fein & Szut, 1982; Hárosi, 1994). The visual pigments of rod photoreceptors (rhodopsin or RH1) absorb light primarily in the green wavelengths, with peak absorbance around 500-530 nm (Hárosi, 1994; Novales Flamarique, 2005). Cone visual pigments absorb maximally in either the ultraviolet wavelengths (SWS1 opsin; range 347-383 nm), short wavelengths (SWS2 opsin, range: 397-482 nm), middle wavelengths (RH2 or MWS opsins, range: 490 to 553 nm), or long wavelengths (LWS opsin, range: 501-573 nm) (Carleton et al., 2020; Hárosi, 1994; Novales Flamarique, 2005).

1.2.2. Colour vision in fishes

Colour vision is the ability of an organism to discriminate between different wavelengths of light regardless of its intensity (Levine & MacNichol, 1982). A minimum of two photoreceptor types, each containing a different visual pigment, are required for colour discrimination (Fein and Szuts, 1982; Hárosi, 1994). Colour vision in fishes is thought to be widespread, which is based on the multiplicity of visual pigments encountered in the retinas that have been examined—with most species having two or more cone visual pigments (Levine & MacNichol, 1982; Marshall et al., 2019). Variability in visual pigment types among species is great with some fishes, like catfishes, having only two cone visual pigments and some tropical fishes having up to thirteen (Carleton et al., 2020; Levine & MacNichol, 1982).

Colour vision can be modulated by differential expression of opsin types either as a function of retinal location (Dalton et al., 2017; Savelli & Novales Flamarique, 2018; Savelli et al., 2018) and/or developmental stage (Hoke et al., 2006; Savelli et al., 2018). The former allows for simultaneous optimal sensing of varying backgrounds line of sight and the latter allows for plasticity to tune the visual system throughout the life history of the animal, which often involves changes in photic habitat (Carleton et al., 2020; Dalton et al., 2017; Hoke et al., 2006; Savelli et al., 2018).

Many fishes possess an ultraviolet cone that extends the animal's visual range below 400 nm. This cone type is often found among planktivorous fishes (Browman et al., 1994; Loew et al., 1993; Novales Flamarique, 2013, 2016) where it is thought to improve the contrast of zooplankton as part of the fishes' colour-vision system (Novales Flamarique, 2013, 2016). Ultraviolet cones have also been found among non-planktivorous fishes where they may be involved in other functions such as mate selection and communication (Cummings et al., 2003; Novales Flamarique, 2013; Siebeck et al., 2010).

1.2.3. Polarization vision of anchovies

While colour vision relies on the wavelength of light to obtain information from the environment, the polarization of light (i.e., the orientation of the electric field) can also be used to enhance the animal's vision for ecological purposes (Labhart, 2016). Many invertebrate visual systems are polarization-sensitive (Labhart, 2016), but among vertebrates, it is only for the northern anchovy that polarization sensitivity and the photoreceptor basis for this capacity have been conclusively demonstrated (Novales Flamarique, 2019).

In these fishes, polarized light vision is mediated by two types of axially dichroic photoreceptors with orthogonal polarization sensitivity (Novales Flamarique 2017). These cones possess lamellae that run parallel to the length of the photoreceptor, making them differentially sensitivity to the orientation of the electric field (Fineran & Nicol, 1976, 1978; Novales Flamarique & Hárosi, 2002**;** Novales Flamarique, 2017), in a similar fashion to the invertebrate rhabdomeric system (Labhart, 2016). Polarization sensitivity allows the northern anchovy to detect zooplankton at longer distances than if foraging under unpolarized light (Novales Flamarique, 2019).

1.3. Zooplankton ecology and morphology

1.3.1. Orientation and migration of zooplankton

Zooplankton are a diverse group of pelagic animals that are the main food source for many marine and freshwater fishes (Brierley, 2014; Hays, 2003; Lampert, 1989). Zooplankton live in vertically stacked communities in the water column wherein different depths can contain vastly different species (Benoit-Bird, 2009; Brierley, 2014). Zooplankton undertake diel vertical migrations that involve upward movement at dusk and downward displacement at dawn in an effort to avoid predation (Brierley, 2014; Hays 2003).

Multiple studies have shown that several species of fish with life stages that feed on zooplankton (e.g., salmonid fishes) have peaks of consumption during crepuscular periods (Lampert, 1989). There are two properties of the crepuscular light spectrum that stand out compared to the spectrum throughout the day. First, the proportion of ultraviolet light (with respect to the total intensity) is at its maximum. Second, downwelling light is at its greatest polarization—with up to 67% measured in coastal waters (Novales Flamarique & Hawryshyn, 1997). These changes in the characteristics of light could be used by some fish species with enhanced ultraviolet or polarization sensitivity to improve their foraging performance on zooplankton (Novales Flamarique, 2013, 2019).

1.3.2. Exoskeleton of zooplankton

In part to protect against predation, many zooplankton taxa have evolved a hard exoskeleton often consisting of chitin or calcium carbonate matrices (Otte et al., 2014; Hessen et al., 2000). The constituents of their exoskeletons are dependent on the biochemical signature of the environment that the zooplankton lives in (Alstad et al., 1999; Hessen et al., 2000).

Zooplankton exoskeletons vary widely in morphology and overall appearance in the visible spectrum (λ range: from 400-760 nm), at least to a human observer. There is a general trend toward increased translucency with decreasing size of zooplankton. For instance, small copepods (less than 3 mm in size) are often more translucent than larger

zooplankton (e.g., amphipods), though even large species may show great translucency throughout much of their bodies (e.g., mysids, euphausiids) (Bagge, 2019**;** Cronin, 2016; Neville, 1975). Translucency can nevertheless vary widely for a given individual depending, for instance, on whether the digestive system contains opaque food items (Cowles 2014). Other, structural features, such as eyes and their pigmentation can also reduce translucency of zooplankton and improve their conspicuousness to predators (Cronin, 2016).

Some zooplankton have evolved exoskeletons that can make them invisible to predators at particular angles of incident light. This is the case for some parasitic copepods in the genus *Sapphirina* whose exoskeletons reflect solely ultraviolet light at high angles of incidence (Gur et al., 2015). Such reflectance is invisible to non-UV sensitive organisms (Silberglied, 1979). It is believed that the UV reflectance by Sapphirinids is part of a courting “dance” ritual, which also involves rapid changes in colour in the visual part of the spectrum (Titelman et al., 2007; Gur et al., 2015).

1.3.3. Optical properties of zooplankton

Daphnia and other zooplankton that fish consume are optically anisotropic in that they will change the intensity, colour and polarization of light that traverses or reflects from their bodies (Novales Flamarique & Browman, 2001). The presence of lipid sacs (Gallager and Mann, 1986) and optical properties of ingested materials often determine the transmittance of light through zooplankton. Structural properties of the cuticle can also contribute to the characteristics of light emanating from the zooplankton by altering its reflectance, predictably. For instance, when cuticular layers have an order that resembles a quarter wave multilayer stack of alternating dielectrics (Figure 1.5), it is possible to approximate measured reflectance by applying Fresnel’s laws to the multilayer stack (Land, 1966; Gur et al., 2015). Other zooplankton, including Sapphirinids, may have alternating stacks of dielectric and cytoplasm that may approximate the quarter-wave conditions (Baar et al., 2014) but their optical properties have not been explored.

1.4. Thesis objectives

This thesis aims to contribute to our understanding of how light cues from zooplankton and retinal mechanisms potentially used by zooplanktivorous fishes are used to perceive zooplankton. Given the lack of information on the reflectance of zooplankton and its relevance to detection by fishes, my objectives were twofold:

- to measure the spectral reflectance of different species of zooplankton, and
- to model the contrast of zooplankton to the visual system of two fishes (rainbow trout and zebrafish) in an ecological framework

1.5. Figures

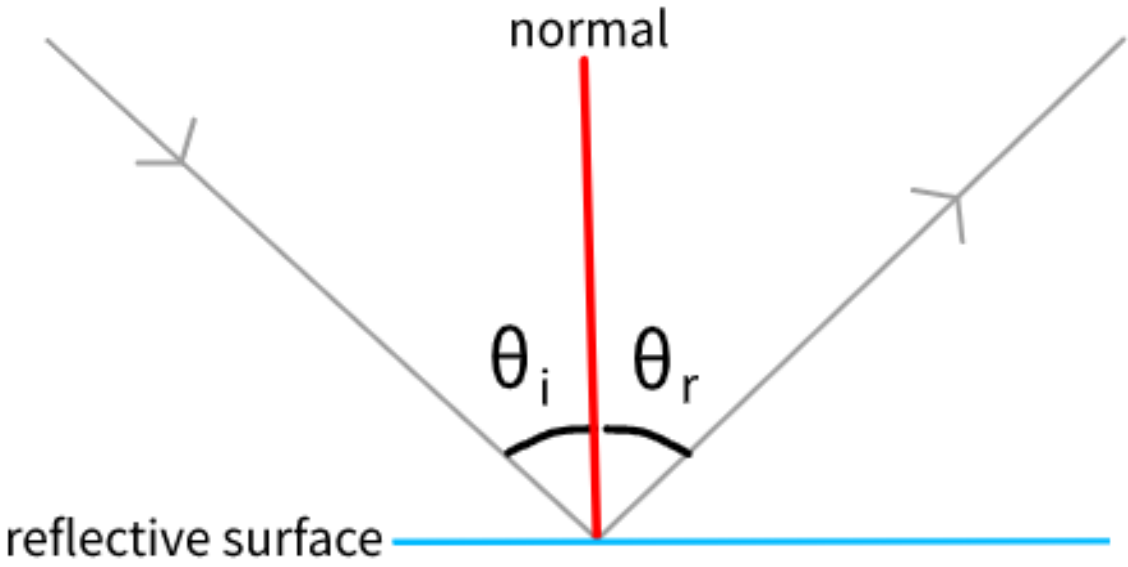

Figure 1.1 **Law of reflection at a smooth (non-diffusive) surface. The angle of the reflected ray (θ_r) upon an incident ray (grey arrows indicate direction) hitting a reflective surface (blue) is equal to the angle of the incident ray (θ_i) that bounces off the reflective surface, i.e., θ_i equals θ_r with respect to the normal (red).**

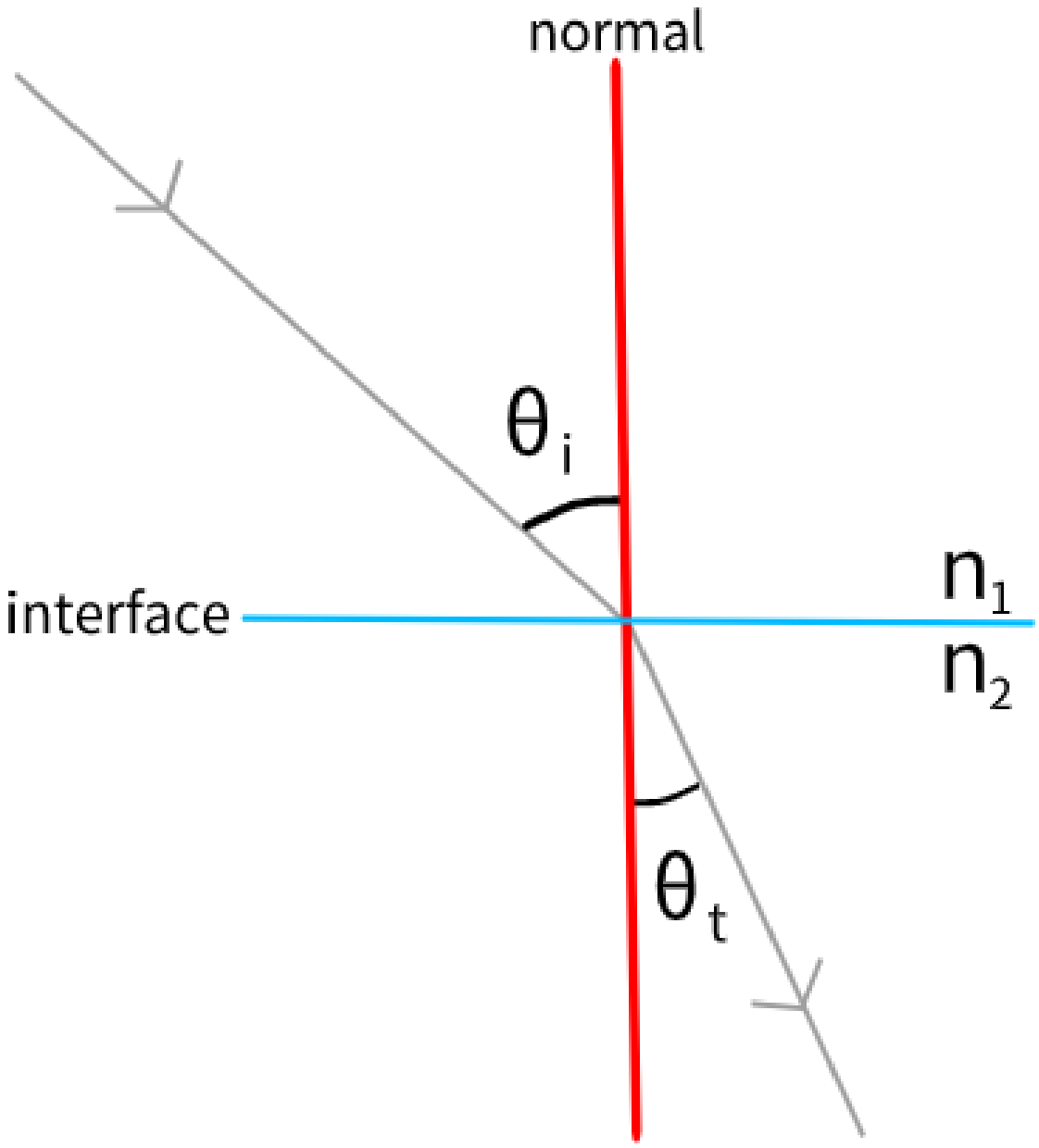

Figure 1.2 **Snell's law or the law of refraction at a smooth (non-diffusive) surface. A ray of light (grey) passes through medium 1 (with a refractive index of n_1) and then passes through medium 2 (with a refractive index of n_2). Once past the interface (blue), the light refracts. The new angle (θ_t) of the refracted light in relation to the normal (red) can be computed by Snell's law using the angle of incident light (θ_i) and the refractive indices of the two media.**

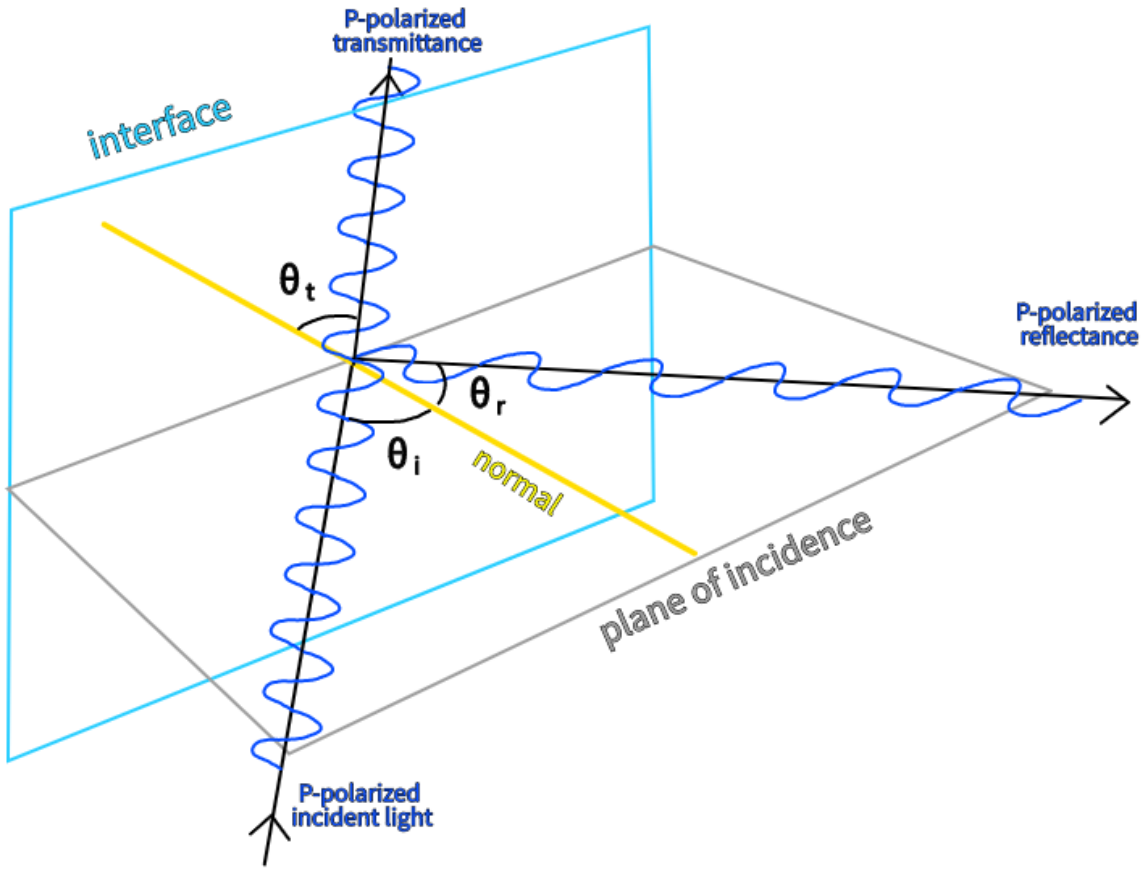

Figure 1.3 **The electric field of P-polarized light (blue) is within (or parallel to) the plane of incidence (grey).**

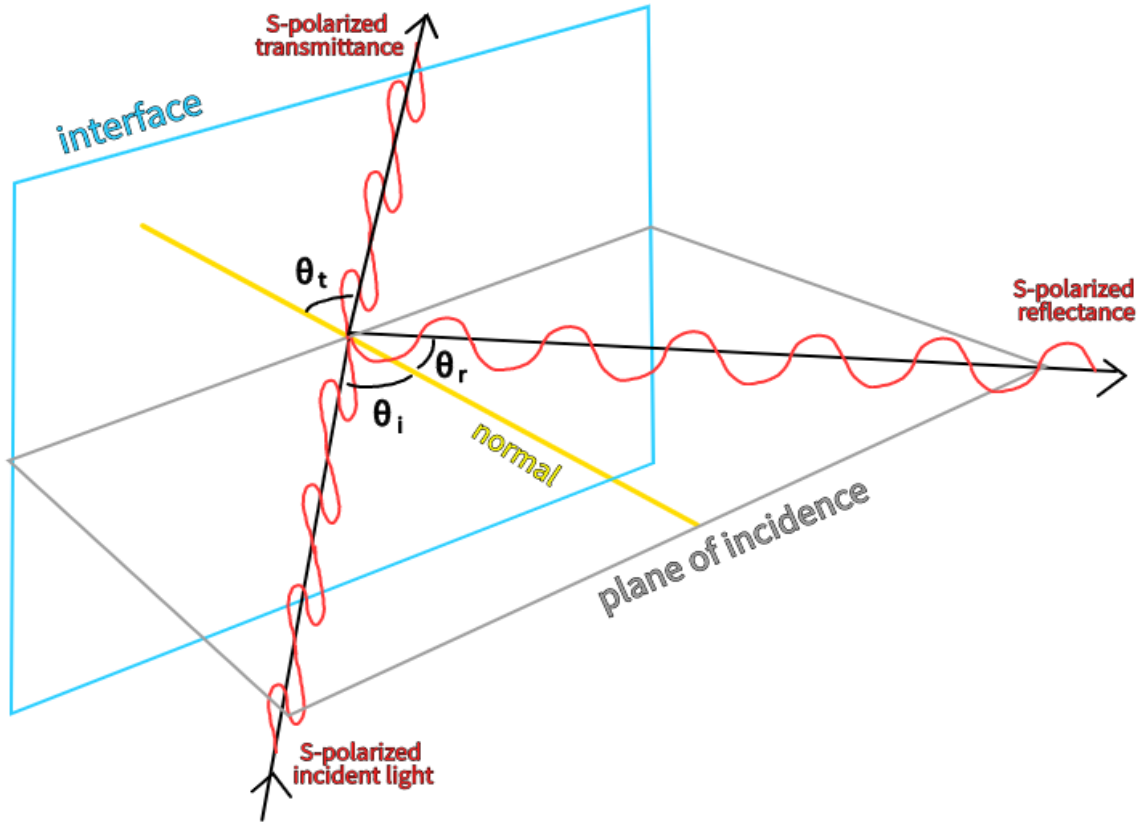

Figure 1.4 **The electric field of S-polarized light (red) is perpendicular (or vertical) with respect to the plane of incidence (grey).**

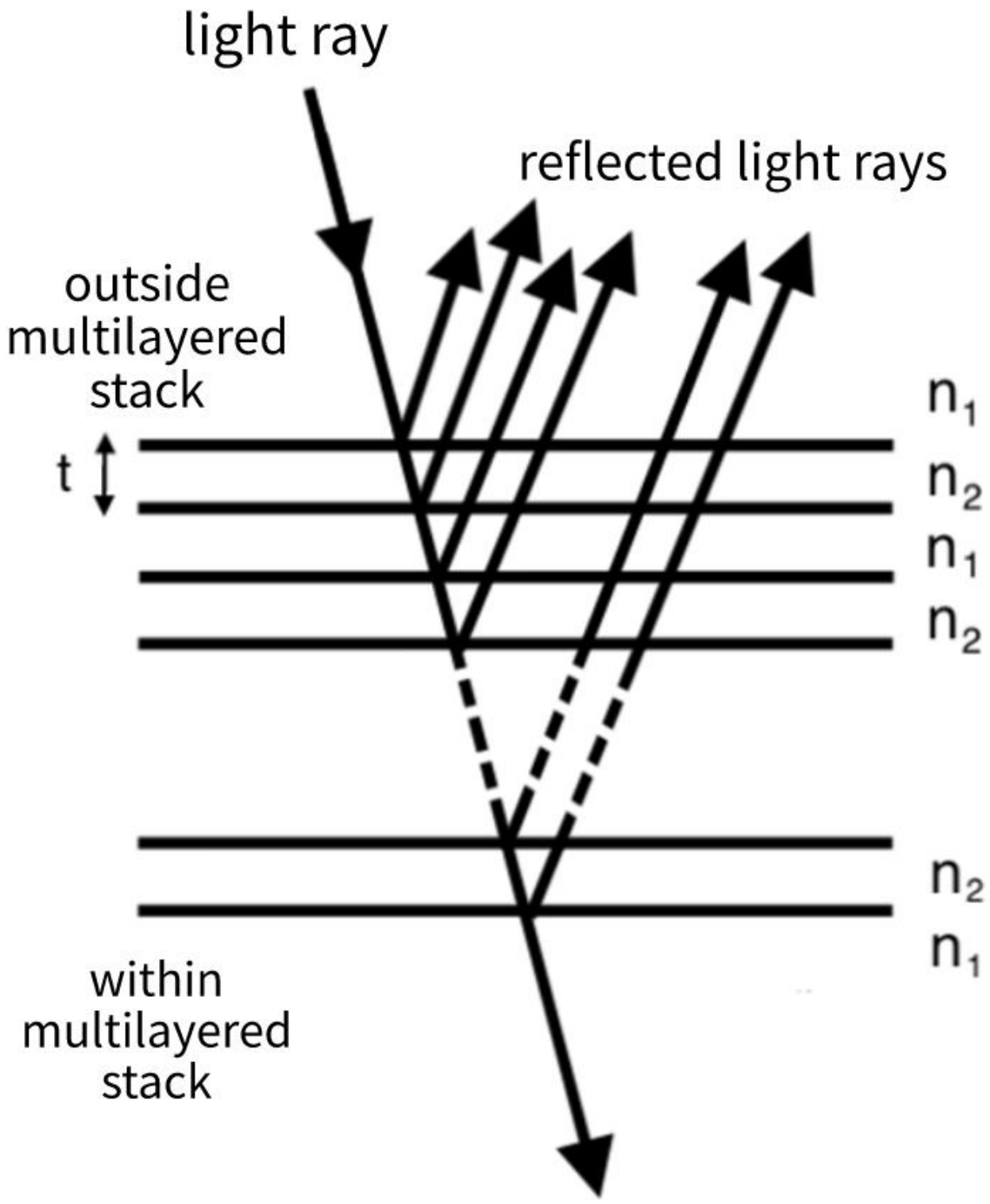

Figure 1.5 **Diagram of a multilayer quarterwave stack wherein incoming light (downward arrow) is reflected (upward arrows) by each alternating layer (of refractive indices n_1 or n_2) as it is transmitted through the numerous layers (dotted lines). The thickness for each layer is designated by t.**

Chapter 2.

Reflectance and absorbance of three zooplankton species

2.1. Introduction

Zooplankton are a broad group of organisms that are prey to many species of fishes. Many zooplankton are small-sized and translucent, which makes them challenging to detect except at very short distances (Novales Flamarique, 2016). In the open ocean this makes most zooplankton essentially invisible when located farther than about 50 cm from the observer. Despite this, many fishes are zooplanktivorous throughout their lives, or have larval/juvenile stages that feed on zooplankton. Zooplanktivorous fishes are visual predators that rely on visual cues (e.g., colour, polarization, prey movement) to detect zooplankton within distances similar to their own body lengths (Novales Flamarique, 2016; Zukoshi et al., 2018).

The optical properties of zooplankton have not been measured with precision due to many factors including their small size and handling challenges. The question of whether different regions of the ambient light spectrum used for vision (range: 320-760 nm) can facilitate perception of zooplankton by fishes has not been explored in detail. This is partly due to the paucity of precise optical measurements concerning zooplankton reflectance in the literature. Previous studies determined the reflectance of *Daphnia* and *Sapphirina* zooplankton (Rick et al., 2012, Gur et al., 2015). However, these studies did not measure the reflectance of individual zooplankton, or for different polarizations of light. It is presently unclear how different parts of the electromagnetic spectrum are contributing to the visual contrasts of zooplankton as perceived by the visual system of fishes in scenarios that include natural light spectra.

Since UV cones are present in the retinas of zooplanktivorous fishes, it has been hypothesized that UV light might reflect off prey zooplankton and might constitute an important component of the total reflectance from the prey. This additional reflected UV light might enhance the contrasts of zooplankton as perceived by two well-characterized visual systems belonging to the rainbow trout (*Oncorhynchus mykiss*) and that of the

zebrafish (*Danio rerio*) (Novales Flamarique & Wachowiak, 2015; Novales Flamarique, 2016). Moreover, it has been hypothesized that the exoskeletons of prey zooplankton reflect naturally occurring UV light, playing a role in UV-based perception of zooplankton by UV-sensitive fishes (Novales Flamarique, 2013, 2016). This hypothesis has been supported by additional experiments with zebrafish larvae wherein their UV sensitivity was shown to be essential in catching prey (Zimmermann et al., 2018).

Here, the reflectance and transmittance of live individuals from three zooplankton species (*Daphnia magna*, *Sapphirina nigromaculata*, and *Heptacarpus sitchensis)* were measured using an optical system equipped with an integrating sphere. From these measurements, contrast calculations were computed by incorporating light measurements from the environment (up to 16 meters in depth), as well as the photon catch of the various cone photoreceptor types found in rainbow trout and zebrafish.

2.2. Materials and Methods

2.2.1. Zooplankton

Three species of zooplankton were used for optical measurements: *Daphnia magna* (a cladoceran; Figure 2.1A), *Sapphirina nigromaculata* (a sapphirinid; Figure 2.1B), and *Heptacarpus sitchensis* (a hippolytoid shrimp; Figure 2.1C). The identities of *D. magna, H. sitchensis,* and *S. nigromaculata* were based on their general morphology (Haney et al., 2013; Cowles, 2014; Razouls et al., 2021). The sapphirinids were obtained from the west coast of Vancouver Island using zooplankton tows carried out by Moira Galbraith of the Department of Fisheries and Oceans (Canada). The *H. sitchensis* arose from shore sampling with a zooplankton net near Victoria (British Columbia, Canada) and the *D. magna* were obtained from a laboratory culture at Simon Fraser University. Sample sizes for each species were: *D. magna* (8), *H. sitchensis* (3), and *S. nigromaculata* (2).

2.2.2. Optical setup for in-vivo light measurements

The optical setup (Figure 2.2A) consisted of the following: a xenon light source (Thorlabs), three apertures, a rotatable linear polarizer, an integrating sphere (Labsphere), a sample holder (Figure 2.2B), metal cell (Figure 2.2C), a condensing lens, a spectroradiometer (Oriel MS260i, Newport, USA), and a desktop computer (Samsung).

A separate computer, LED, camera, and lens setup (Figure 2.2A) allowed for the visualization and adjustment of the zooplankton when it was inserted into the integrating sphere. This was done by adjusting the position of the sample holder, ensuring that the light hit the sample's thorax and did not extend beyond the carapace.

As seen in Figure 2.2A, a beam of light was emitted from the light source and focused by three apertures into an approximately 50 mm diameter beam. The rotatable linear polarizer had been removed and the beam remained unpolarized, passing through a condensing lens—narrowing it further—before entering the integrating sphere. For polarized light measurements, the linear polarizer was kept in place (refer to section 3.2).

The integrating sphere had four openings: a front port, a back port, a top port wherein the sample holder could be inserted, and a side port where an optic fibre was attached into the sphere to allow for the exit of light and its measurement (photon counts) by the spectroradiometer (Figure 2.2A). Both the front and back ports had covers that could be affixed to their respective ports, but the front port's cover had a small hole in the centre so that light could enter the sphere. The top port possessed a slot to insert the sample holder and could be rotated in the azimuth plane. The sample holder was equipped with a slot to insert a metal cell that immobilized the zooplankton sample (Figure 2.2B). The sample holder had openings on both the sides of the metal cell's slot, allowing light to pass through. The cell (Figure 2.2C) consisted of two square metal pieces with a large circular glass coverslip affixed to the centre of each piece. Silica glass cover slips (refractive index of 1.52) were affixed to these windows, allowing the sample to be viewed from either side of the cell. Four metal screws were tightened on each of the four corners of the metal cell to immobilize the sample (zooplankton) alive. The zooplankton was immersed in water within the metal cell by means of a rubber O-ring (Figure 2.2C).

2.2.3. Reflectance and absorbance recordings

Reflectance was measured for the range 320 to 740 nm using an imaging spectroradiometer. Reflectance measurements were acquired for each zooplankton at five different azimuth angles relative to the normal to the plane of the specimen holder:

5º, 15º, 25º, 35º, and 45º. These angles span a range of potential incident rays that would be incident on the zooplankton in nature.

During measurements of reflectance, photons not reflected by the test sample would be transmitted through the zooplankton and exit through the back port (Figure 2.3). Conversely, all reflected light would be contained within the integrating sphere, undergoing diffuse reflections off the sphere's interior surface, and measured by the spectroradiometer (Figure 2.2A). It has been shown that the front and back ports do not affect the amount of retained reflected light within the integrating sphere because they are small compared to the total size of the sphere (Taylor, 2013).

For each set of measurements at a specific angle of incidence, reflectance was calculated as follows (Equation 2):

$$R\% = \frac{sample - reference}{total\ reference - noise} \cdot 100\% \quad (2)$$

Where *R%* is the relative reflectance of the zooplankton at a specific angle, expressed as a percentage, *sample* is the photon count from the ensemble of the zooplankton, cell, and water at a specific angle; *noise* is the baseline photon count or Poisson noise from the electrical equipment; *reference* is the photon count from the combination of cell and water (i.e., without the specimen; and *total reference* is the photon count of incident light entering the integrating sphere (with the back port closed during measurements).

In the case of absorbance measurements (Figure 2.4), the back port of the integrating sphere was closed. Absorbance (A) was calculated as follows (Equation 3):

$$A = \log_{10} \frac{reference - noise}{sample - noise} \quad (3)$$

Where: *sample* is the photon catch from the combination of zooplankton, water, and cell; *reference* is the photon catch of just the water and cell (without the zooplankton); and *noise* is the photon count from Poisson noise readings (no visible light entering the sphere).

Transmission was computed as (Equation 4):

$$T = 10^{-A} \quad (4)$$

Wherein *T* is the transmittance of light through the sample, and *A* is the absorbance of light by the sample.

2.2.4. Setup modification for polarization measurements

The setup used for reflectance measurements with unpolarized light was adjusted to measure polarized reflectance. A rotatable linear polarizer was inserted between the light source and the integrating sphere (Figure 2.2). The polarizer was held within a rotatable mount that allowed for adjustments to the transmission axis. Polarized reflectance measurements were obtained with the transmission axis of the polarizer in either the horizontal or vertical directions, corresponding to P-polarized (Figure 1.3) and S-polarized light (Figure 1.4) orientations. Equation 2 was used to calculate reflectance. Reflectance measurements using polarized light were performed following the same measurements using unpolarized light. Thus, all measurement parameters remained the same expect for the polarization of incident light. Lastly, ANOVA and standard error statistics were applied to the three polarization groups.

2.2.5. Contrast calculations

To compute the theoretical visual contrast of a zooplankton by a fish species, the following parameters are required: 1) the reflectance spectra of the zooplankton; 2) the transmittance spectra of the zooplankton; 3) the photoreceptor absorptance of the fish's visual system; and 4) the spectral irradiances from the environment.

A set of underwater spectral irradiance data (Figure 2.5) was obtained at various depths in Cowichan Lake (BC, Canada; Novales Flamarique et al., 1992). This oligotrophic freshwater lake reaches depths of up to 150 meters and is host to a variety of fishes including salmonids like rainbow trout (The BC Lake Stewardship Society, 2014). The irradiances measured in Lake Cowichan consisted of downwelling and sidewelling irradiances components. The sidewelling (horizontal) "sun" measurements were taken in the azimuth direction containing the sun and the "antisun" measurements were acquired in the opposite direction (Figure 2.6).

To calculate the theoretical contrast that would be perceived by the fish, the absorptance of its cone photoreceptors was computed as (Equation 5):

$$absorptance = 1 - 10^{(absorbance)(S)(l)} \quad (5)$$

Where, for a specific cone type, *S* is the transverse specific density, and *l* is the average outer segment length. The absorbance of visual pigments in both rainbow trout and zebrafish were previously measured by microspectrophotometry as were the *S* and *l* parameters of all photoreceptor types (Novales Flamarique, 2013, 2016; Novales Flamarique & Hawryshyn, 1997). The maximum wavelength of absorbance (λ_{max}) of cone visual pigments in rainbow trout were: 390 nm (UV), 443 nm (S), 501 nm (M), 540 nm (M), and 565 nm (L), and 620 nm (L). In zebrafish, these were: 360 nm (UV), 420 nm (S), 498 (M), and 564 nm (L) (Novales Flamarique, 2013, 2016).

Each cone's visual pigment absorptance data were multiplied by the reflectance of the *Daphnia* and the downwelling irradiances (Figure 2.5), yielding the reflected photon catch for each cone type at each depth analyzed (i.e., 3.3, 6.6, 10, 13.3, and 16.6 metres). The absorptances were separately multiplied by the transmittance data of the *Daphnia* and the horizonal irradiances—sidewelling irradiances from either the sun or antisun directions (Figure 2.5)—yielding the transmitted photon catch for each cone type at each depth in the sun and anti-sun directions.

The total photon catch of a given cone type emanating from the zooplankton light cues was then the sum of the reflected photon catch and the transmitted photon catch. The zooplankton contrast was computed as (Equation 6):

$$Contrast = \frac{\left|P_{Daphnia} - P_{Background}\right|}{\left|P_{Daphnia} + P_{Background}\right|} \quad (6)$$

Where $P_{Daphnia}$ and $P_{background}$ are the photon catches from a given cone interaction.

The cone interactions evaluated were: L–M, UV–M, S–M, UV–L, S–L, UV–(L–M), S–(L–M), UV–(L+M), S–(L+M), (UV–S)–(L–M), and (UV–S)–(L+M). These cone interactions comprise all possible combinations of cone mechanisms that could theoretically yield a retinal signal at the level of the ganglion cells (the output of the

retina). Evidence for some of these interactions has been obtained by electrophysiological recordings and behavioural experiments (Coughlin & Hawryshyn, 1994; Fratzer et al., 1994; Hughes et al., 1998; Novales Flamarique, 2013; Risner, 2006). In the above interactions of cone mechanisms, the photon catch of each cone type was multiplied by its relative frequency with respect to others in the retina. In the zebrafish retina, M and L cones are twice as frequent as UV and S cones. In the rainbow trout retina, the density of all cone types is approximately the same at the zooplanktivorous stages of interest.

2.3. Results

2.3.1. External morphology

The three species of zooplankton showed different morphology and colour appearance to the human eye (Figure 2.1). The *Daphnia magna* was translucent, with a yellow-tinted cuticle and a green digestive tract, from ingest algae (Figure 2.1a). In contrast, *Sapphirina nigromaculata* was more colourful with prominent cyan, blue, and purple patches (Figure 2.1b). The urosome was blue-pink at the posterior tip. The shrimp, *Heptacarpus sitchensis*, had a digestive tract that appeared yellow-green (likely due to ingested algae), but was generally translucent except for the cephalothorax which was dark green (Figure 2.1c).

2.3.2. Reflectance

The overall trend in reflectance with angle of incidence was the same between zooplankton species with greater values associated with lower angles of incidence (Figures 2.8-2.10). Reflectance was greatest in the longer wavelengths ($\lambda > 580$ nm) and smallest in the shorter wavelengths ($\lambda < 420$ nm), with *Sapphirina* having the largest reflectance of all the three species (Figure 2.9). Despite these differences, ANOVA and standard error (Figure A1) showed that the reflectances between the three polarization groups were not significantly different.

When illuminated by unpolarized light, the reflectance spectrum of *Daphnia* was broad, spanning from the ultraviolet to the visible spectrum—with a maximum in the long wavelengths (λ > 580 nm), and a secondary maximum in the middle wavelengths, i.e., in the range: 450 – 570 nm (Figure 2.8A). The same trend was found when the incident light was linearly polarized, i.e., either parallel to the plane of incidence (P-component, Figure 2.8B) or perpendicular to the plane of incidence (S-component, Figure 2.8C). Because of the small number of measurements, P and S-polarized reflectances were not statistically different at any angle of incidence.

Whether illuminated by polarized or unpolarized light, the reflectance of *Sapphirina* was also highest in the longer wavelengths, i.e., λ > 580 nm (Figure 2.9A). In comparison with *Daphnia*, its reflectance in the UV (λ < 400 nm) was, overall, 15% greater**.** As opposed to that of *Daphnia* and *Sapphirina*, the reflectance of *H. sitchensis* was broader, with two similar humps spanning the range 360 to 400 nm and 470 to 580 nm (Figure 2.10A).

2.3.3. Absorbance of *Daphnia magna*

The average absorbance of *D. magna* peaked around 455 nm with another secondary peak between 330 and 370 nm (Figure 2.11). Absorbance values gradually decreased towards zero above 455 nm.

2.3.4. Contrast of zooplankton

For the rainbow trout visual system, the greatest theoretical contrast of *D. magna* arose from the UV–(L–M) interaction in downwelling-antisun conditions at 3.3 m in depth (Table 2.1). The S–(L–M) interaction produced larger contrasts than the UV–(L–M) interaction at greater depths, i.e., 10 metres in downwelling-sun conditions and 13.3 metres in downwelling-antisun conditions. Contrast generally decreased as a function of increasing angle of incidence and with increasing depth. The only exception to this trend was when the cone interaction that yielded the highest contrasts changed in rainbow trout (Table 2.1), i.e., below 10 metres (downwelling-sun) and below 13.3 metres (downwelling-antisun).

When the zebrafish's visual pigments were considered, the greatest contrast arose from the S-2(2L-2M) cone interaction in downwelling anti-sun conditions at 3.3 meters in depth (Table 2.1). Similar to the modeling results for rainbow trout, contrast based on downwelling anti-sun conditions were larger than those based on downwelling sun conditions.

2.4. Discussion

2.4.1. Reflectance spectra of three zooplankton species

The reflectance of zooplankton has only been measured for *Daphnia magna* (Rick et al., 2012) and several tropical *Sapphirina* species (Gur et al., 2015). Measurements by Rick et al. (2012) were carried out using a manually held light source (at approximately 0° incidence) and a detector (at approximately 45°) on *Daphnia* taken out of water and settled on a black cloth. Thus, these measurements lack the optical accuracy to obtain reliable data. The reflectance of *Sapphirina* was carried out with a modified microspectrophotometer, but the species measured are not found in temperate waters and may therefore have different cuticular disposition to the one measured in this thesis.

The reflectance of *D. magna* that was measured at 5° incidence (Figure 2.8A) is similar in overall appearance to that measured by Rick et al. (2012) at normal (0°) incidence. Both results show an increase in reflectance towards the shorter wavelengths (the UV region, $\lambda < 400$ nm), a trough around 425 nm, and an increase in reflectance thereafter, towards the longer wavelengths. Nonetheless, there are slight differences between both curves including the location of the minimum at 425 nm measured by Rick et al. (2012) compared to 410 nm in this study (Figure 2.8A). As well, the reflectance curve in this study increased sharply above 410 nm—plateauing around 450 nm—whereas that of Rick et al. (2012) increased gradually between 425 and 700 nm. The differences in the reflectance spectra are likely due to differences in measurement procedure between studies or the disposition and state of the *Daphnia*.

The lower reflectance values at higher compared to lower angles of incidence may be due to increased absorbance by the sample. At greater angles, the path of light through the specimen increases due to its preferential volume spread perpendicular to the plane of incidence. The lower reflectance resulting from P-polarized in comparison

with the S-polarized illumination of *Daphnia* (Figures 2.8B, C) at 35° and 45° incident light may be explained by Brewster's Law (for review see: Lvovsky, 2013; Ouseph et al., 2001) acting at the level of the cuticle. Given the predicted refractive index value of the chitinous cuticle, 1.62 (Azofeifa et al., 2012), Fresnell's equations (for review, see: Lvovsky, 2013) applied to the water-cuticle interface would result in a Brewster's angle of 50.6°, at which there should be little or no reflectance of P-polarized light. The decrease in reflectance among all zooplankton (Figures 2.8-2.10) as the incident angle of light increases is consistent with the decrease in reflectance at an interface as per Brewster's Law.

Gur et al. (2015) measured the reflectance at various angles of incidence of two Sapphirinid species, *Sapphirina metallina* and *Copilia mirabilis*, and found that the peak reflectance would shift into the ultraviolet range with increasing angle of incidence. Subsequently, Gur et al. (2015) showed that the shifts in reflectance could be predicted from the optical properties of the cuticle, which is a multi-layer structure composed of alternating layers of guanine and cytoplasm meeting the quarter wavelength ideal reflector condition (Land, 1966). In this study, the shift in reflectance towards the UV wavelengths with increasing angle of incidence was not observed. The reasons for this discrepancy between studies are unknown, but it may involve different cuticular composition between species. The thorax of the specimens examined (the target of the incident light had a preponderance of brown pigmentation (Figure 2.1b) which was not present in the specimens examined by Gur et al. (2015). This would preferentially reflect longer wavelengths light and may overpower the structural effects of the cuticle on reflectance.

Additionally, Gur et al. (2016) determined that differences in light adaptation state affected the measured reflectance of Sapphirinids. They found that dark-adapted Sapphirinids reflected more light in the UV wavelengths than light-adapted Sapphirinids. The appearance of the Sapphirinid used in this study (Figure 2.1B) is similar to the light-adapted Sapphirinid used in their study. This lessened UV reflectance by light-adapted Sapphirinids might explain the low reflectance of UV light by *Sapphirina nigromaculata* (Figure 2.9).

2.4.2. Interactions between short and long wavelength-sensitive cones result in higher contrast and improved foraging on zooplankton

Previous studies have demonstrated that the foraging performance of zebrafish and rainbow trout improve when the background illumination contains ultraviolet wavelengths (Novales Flamarique, 2013, 2016). In addition, theoretical calculations that compared interactions between cone mechanism under artificial light conditions showed that the contrast of *Daphnia* to young rainbow trout was greatest for the UV–(L–M) combinations (Novales Flamarique, 2013). This was due to the approximately similar photon catch of the L and M cone mechanisms under the illumination provided by a 150-watt xenon lamp, which has a broad-spectrum emission encompassing ultraviolet wavelengths.

This thesis shows that the same interaction of cone mechanisms (i.e., UV–(L–M)) should provide the greatest contrast for all the zooplankton tested to the visual system of rainbow trout (Table 2.1) under the irradiance conditions found in natural surface waters (<17m). As depth increases, the ultraviolet get filtered out from the available light spectrum such that the S-(L-M) cone mechanism becomes the dominant interaction providing contrast. For the zebrafish visual system, it is always the latter interaction of cone mechanisms that provides the greatest contrast, irrespective of depth. This can be explained by the overall shorter wavelength absorbance of the S cone of zebrafish (λ_{max} at 418 nm) as opposed to that of rainbow trout (λ_{max} at 430 nm). In other words, the S cone of zebrafish has greater photon catch than the UV cone (with λ_{max} at 360 nm) at all depths examined, and this follows from the overlap of the natural irradiance spectrum and the absorbance profile of each cone visual pigment.

The cones of zebrafish and rainbow trout are arranged in lattice formations across the retina (Cheng et al., 2006; Raymond et al., 2014). Double cones express the M and L visual pigments whereas UV and S visual pigments are expressed by independent populations of single cones (Cheng et al., 2007; Novales Flamarique, 2013, 2016). It is the repeatability of the unit mosaic (consisting of double and single cones in specific ratios) that allows for similar chromatic input to higher-order neurons from the target and the background, a situation that favours improved colour contrast and visual acuity (Frau et al., 2020). Experiments on a variety of non-mammalian vertebrates, including fishes, suggest that double cones detect the background illumination whereas

the single cones contain offset visual pigments (from the main wavelengths in the background) and are used as target detectors (Cummings & Partridge, 2001). The results in this thesis lend support to this hypothesis as the highest contrasts were achieved through antagonistic interactions between UV and S cones, on the one hand, and L and M cones, on the other.

2.5. Tables

Table 2.1 Largest theoretical contrasts of *Daphnia* at three angles of incidence (5°, 35°, and 45°) at five depths for the visual systems of rainbow trout (RT) and zebrafish (Z). DS and DAS correspond to downwelling light in the sun and antisun directions, respectively.

Fish Species	Horizontal Irradiance	Depth (m)	5° Incidence		35° Incidence		45° Incidence	
RT	DS	3.3	UV-(L-M)	0.343	UV-(L-M)	0.347	UV-(L-M)	0.308
		6.6	UV-(L-M)	0.329	UV-(L-M)	0.313	UV-(L-M)	0.254
		10	S-(L-M)	0.881	S-(L-M)	0.897	S-(L-M)	0.898
		13.3	S-(L-M)	0.353	S-(L-M)	0.352	S-(L-M)	0.564
		16.6	S-(L-M)	0.132	S-(L-M)	0.125	S-(L-M)	0.096
	DAS	3.3	UV-(L-M)	0.964	UV-(L-M)	0.964	UV-(L-M)	0.955
		6.6	UV-(L-M)	0.630	UV-(L-M)	0.612	UV-(L-M)	0.532
		10	UV-(L-M)	0.627	UV-(L-M)	0.601	UV-(L-M)	0.514
		13.3	S-(L-M)	0.774	S-(L-M)	0.772	S-(L-M)	0.903
		16.6	S-(L-M)	0.461	S-(L-M)	0.447	S-(L-M)	0.383
Z	DS	3.3	S-(2L-2M)	0.226	S-(2L-2M)	0.215	S-(2L-2M)	0.166
		6.6	S-(2L-2M)	0.268	S-(2L-2M)	0.246	S-(2L-2M)	0.183
		10	S-(2L-2M)	0.280	S-(2L-2M)	0.252	S-(2L-2M)	0.179
		13.3	S-(2L-2M)	0.185	S-(2L-2M)	0.161	S-(2L-2M)	0.103
		16.6	S-(2L-2M)	0.120	S-(2L-2M)	0.100	S-(2L-2M)	0.053
	DAS	3.3	S-(2L-2M)	0.643	S-(2L-2M)	0.627	S-(2L-2M)	0.549
		6.6	S-(2L-2M)	0.555	S-(2L-2M)	0.526	S-(2L-2M)	0.433
		10	S-(2L-2M)	0.584	S-(2L-2M)	0.552	S-(2L-2M)	0.455
		13.3	S-(2L-2M)	0.501	S-(2L-2M)	0.466	S-(2L-2M)	0.367
		16.6	S-(2L-2M)	0.400	S-(2L-2M)	0.364	S-(2L-2M)	0.271

2.6. Figures

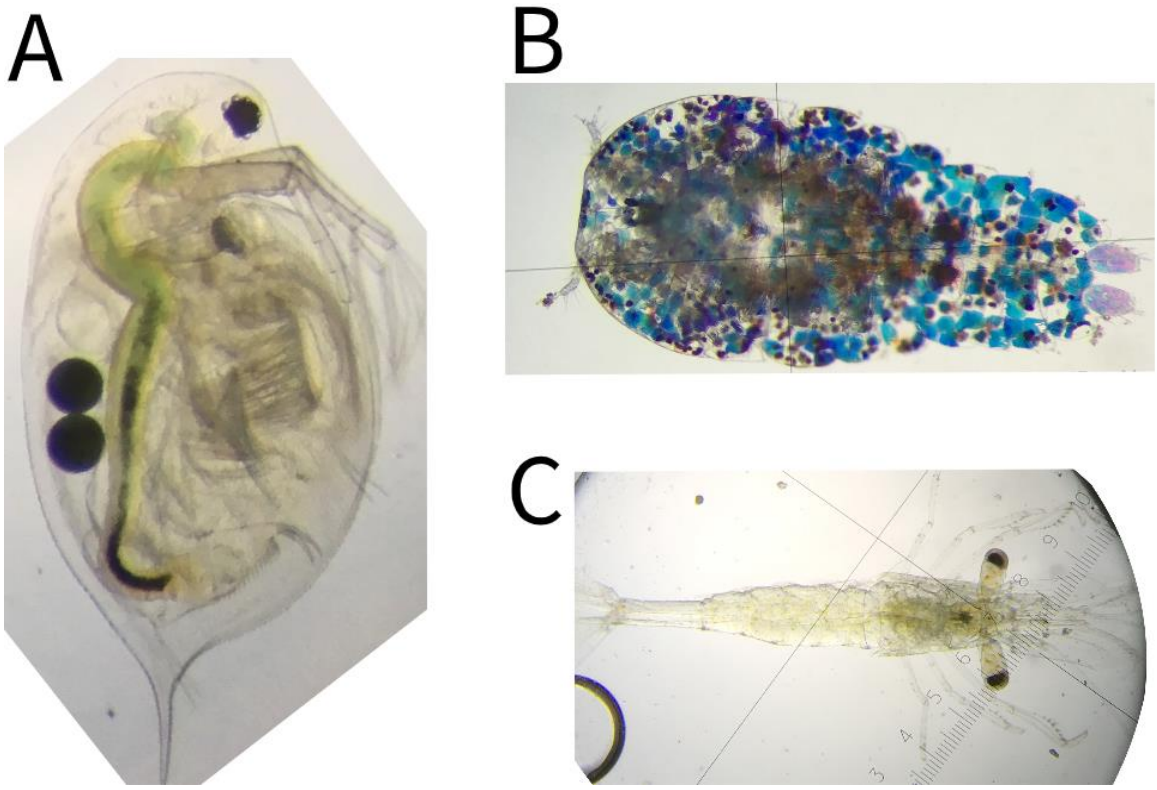

Figure 2.1 **Live zooplankton images of: A) *Daphnia magn*a, B) *Sapphirina nigromaculata*, and C) *Heptacarpus sitchensis*.**

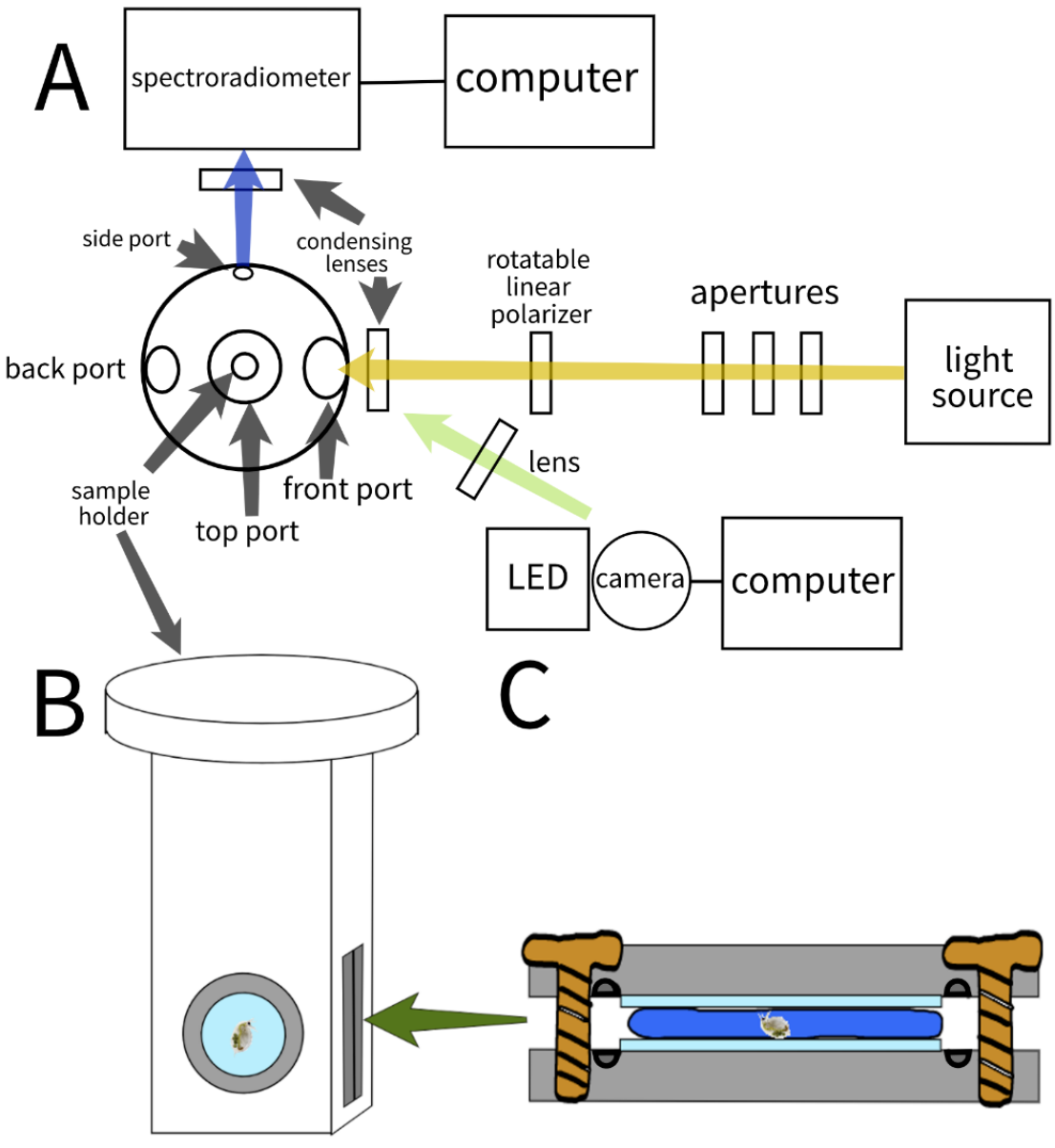

Figure 2.2 **A) Light from the source was focused onto the sample, which was located within a holder inside the integrating sphere. This light was unpolarized, or rendered polarized by the insertion of a rotatable linear polarizer in the optical path. Photon counts were monitored by a spectroradiometer, coupled to the exit port of the integrating sphere, under computer control. B) Illustration of the sample holder containing the cell with a *Daphnia*. The metal cell was inserted (green arrow) into the sample holder of the integrating sphere. C) Side view of the metal cell with a *Daphnia*. The metal plates (grey) and coverslips (light blue) surround the *Daphnia* in water (dark blue). A rubber O-ring fits into the grooves of the metal plates (dark grey semi circles) and encircles the *Daphnia*, keeping the water within the cell. Metal screws (brown) are inserted into each of the four corners of the square metal cell to attach both metal plates together so that the sample is immobilized.**

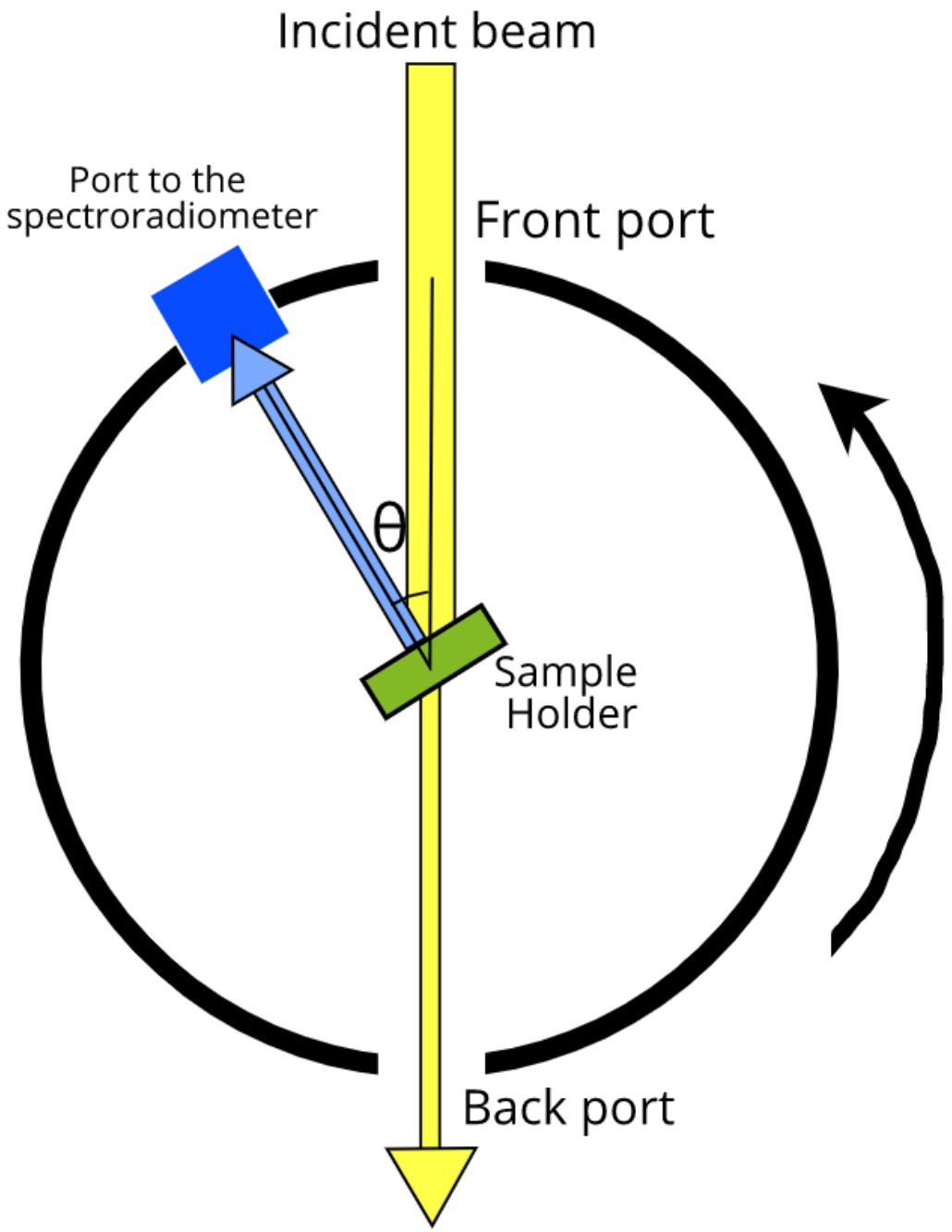

Figure 2.3 **Illustration of reflection measurement set-up. A beam of light (yellow line) enters the integrating sphere through the front port and is incident on the sample holder containing the zooplankon (green). The transmitted component (thinner yellow arrow) exits directly via the back port. Light incidence on the zooplankton at angle θ is partially reflected (blue arrow) and bounces inside the sphere until exiting through a port (blue) connected to the spectroradiometer for measuring photon counts.**

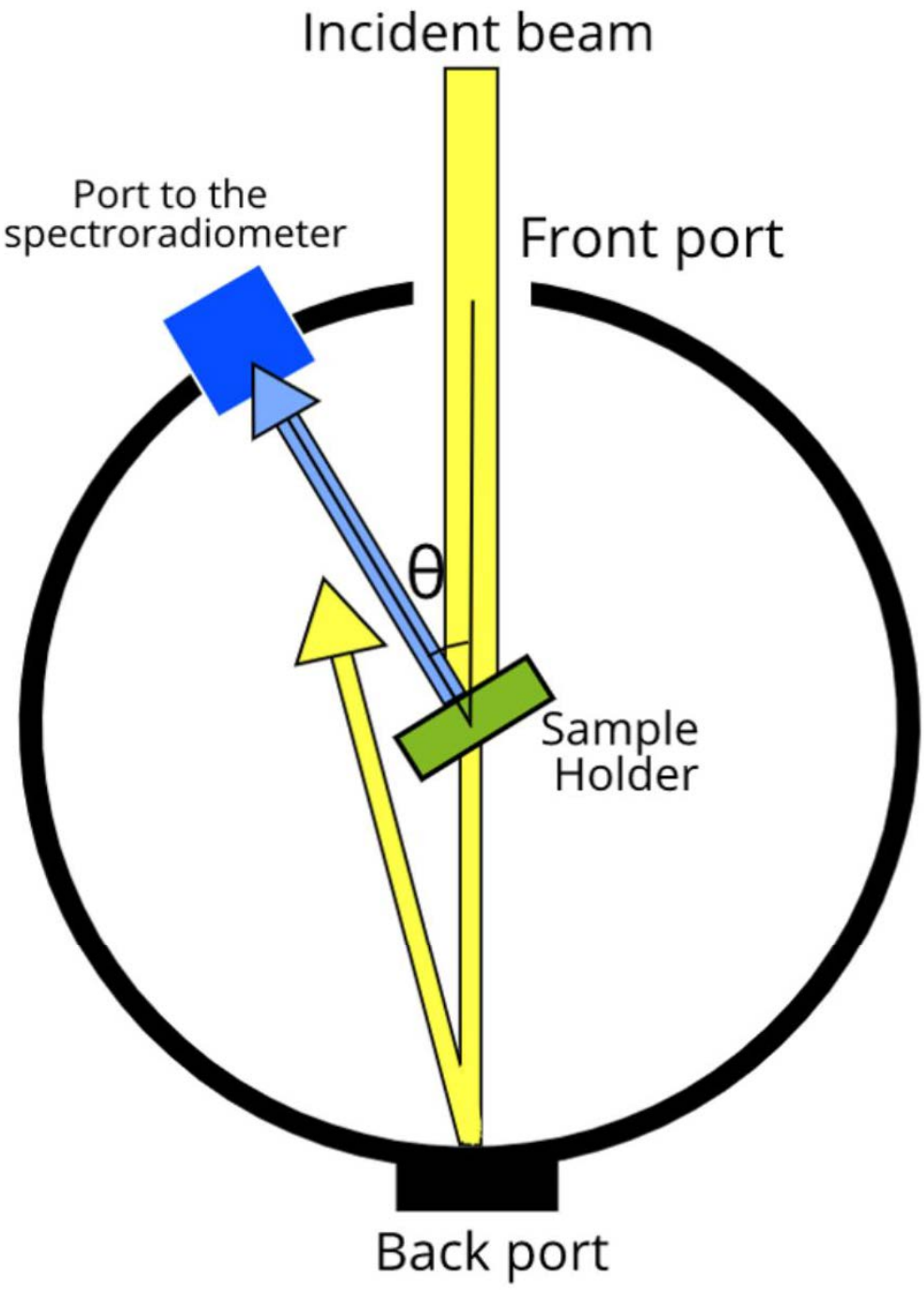

Figure 2.4 **Absorbance measurement set-up. The beam of incident light (yellow line) enters the integrating sphere through the front port and its transmitted and reflected components (thinner yellow arrow and blue arrow, respectively) bounce around the inside walls until reaching the port (blue) connected to the spectroradiometer. The only light not measured is that absorbed by the zooplankton.**

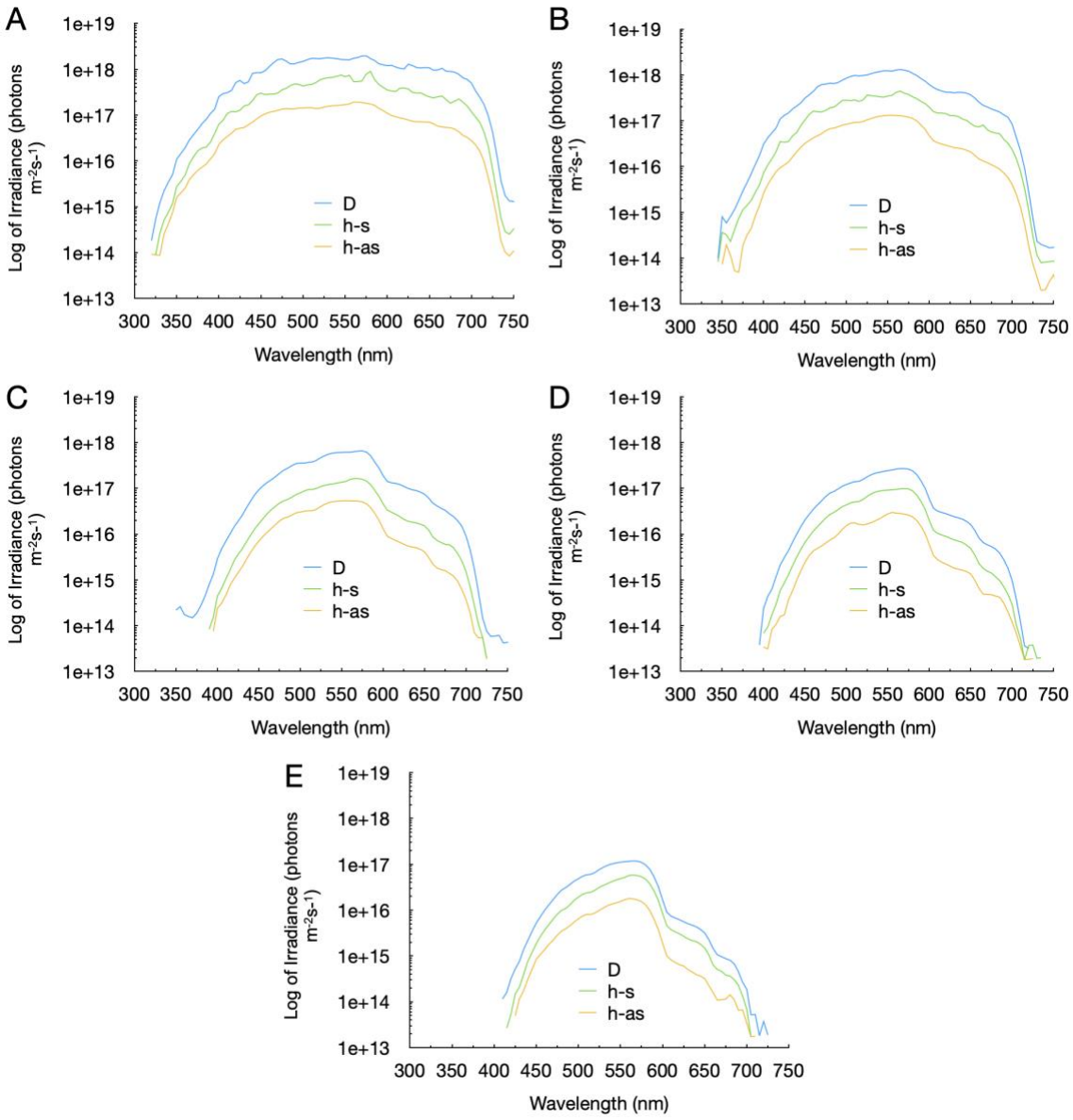

Figure 2.5 **Spectral irradiances from Lake Cowichan (Novales Flamarique et al., 1992) used in the modeling. Measurements taken by SCUBA divers at (A) 3.3 meters depth, (B) 6.6 meters depth, (C) 10 meters depth, (D) 13.3 meters depth, and (E) 16.6 meters depth. The coloured lines indicate downwelling (D) irradiance, horizontal irradiance in the sun direction (h-s), and horizontal irradiance in the antisun direction (h-as).**

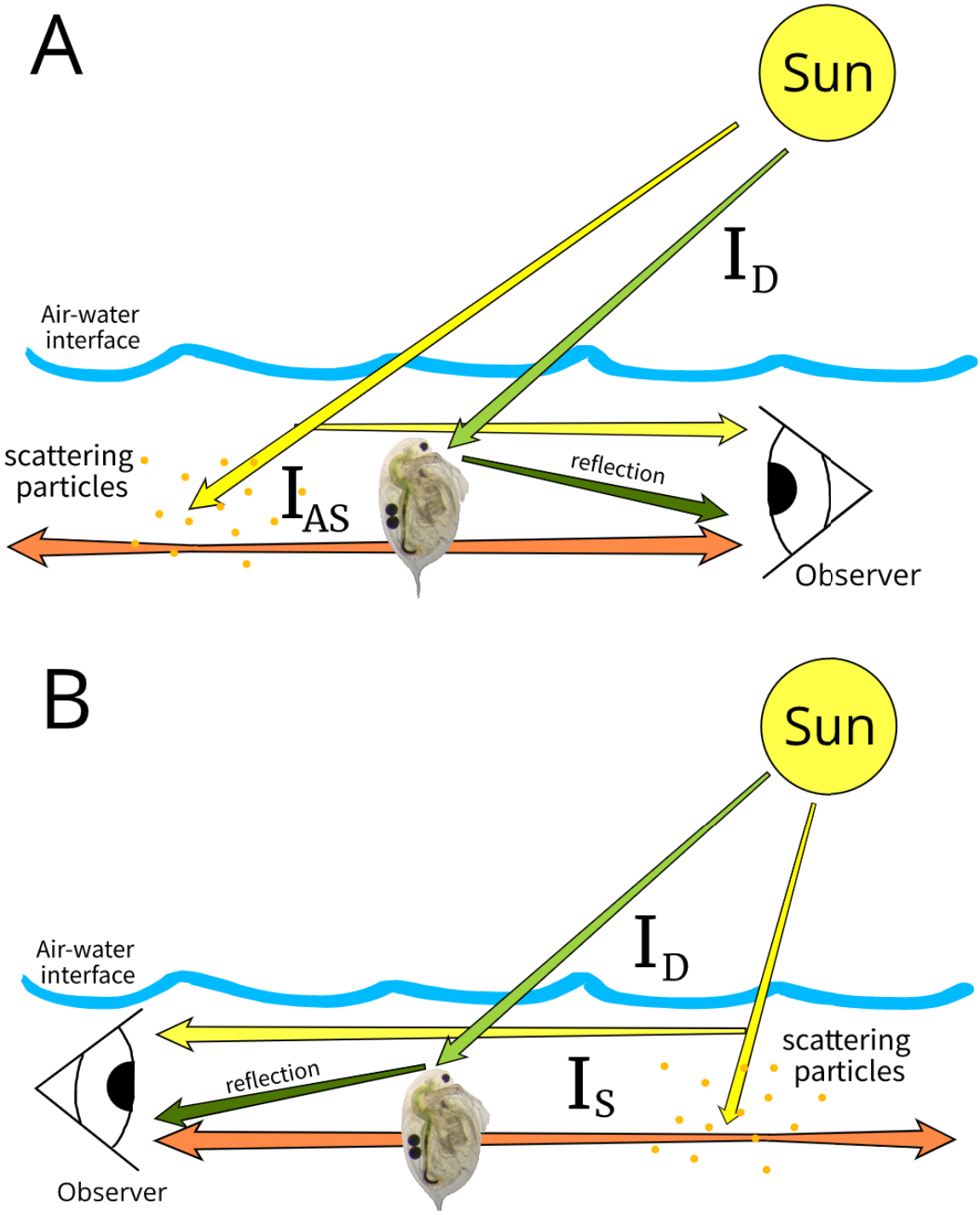

Figure 2.6 **Schematic of main components of light arising from target (*Daphnia*) and background (horizontal yellow arrow) used in the modeling of visual contrast. Light from the *Daphnia* includes components from the background (transmitted through its body, orange arrow) and downwelling light, I_D, reflected from the carapace (green arrows). The fish (observer) views this light against that arising from the background either in the (A) antisun (I_{AS}) or (B) sun (I_S) directions.**

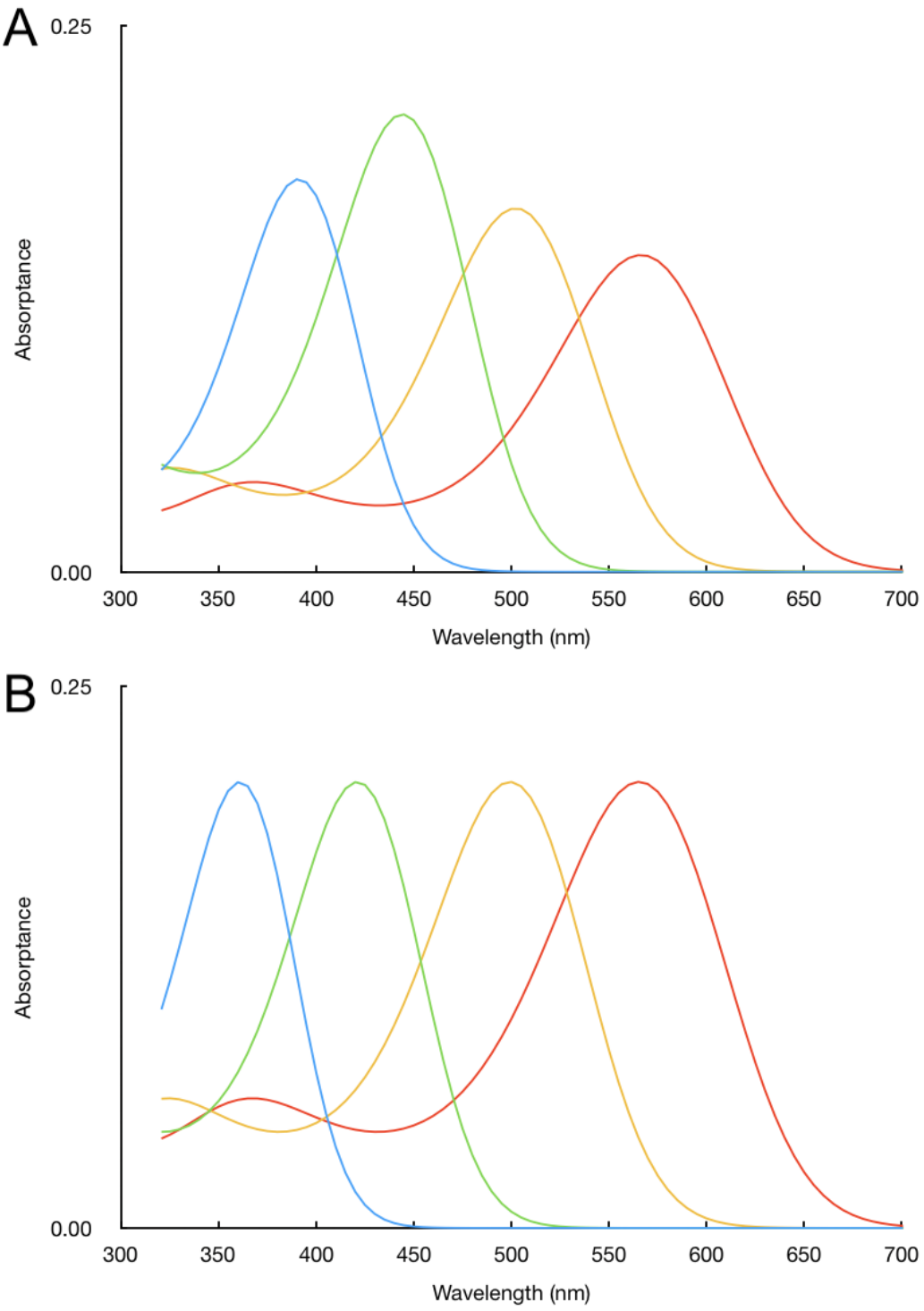

Figure 2.7 **Absorptance values of UV-sensitive (in blue), short-wavelength sensitive (in green), middle-wavelength sensitive (in yellow), and long-wavelength sensitive (in red) cones for the (A) rainbow trout and (B) zebrafish visual systems.**

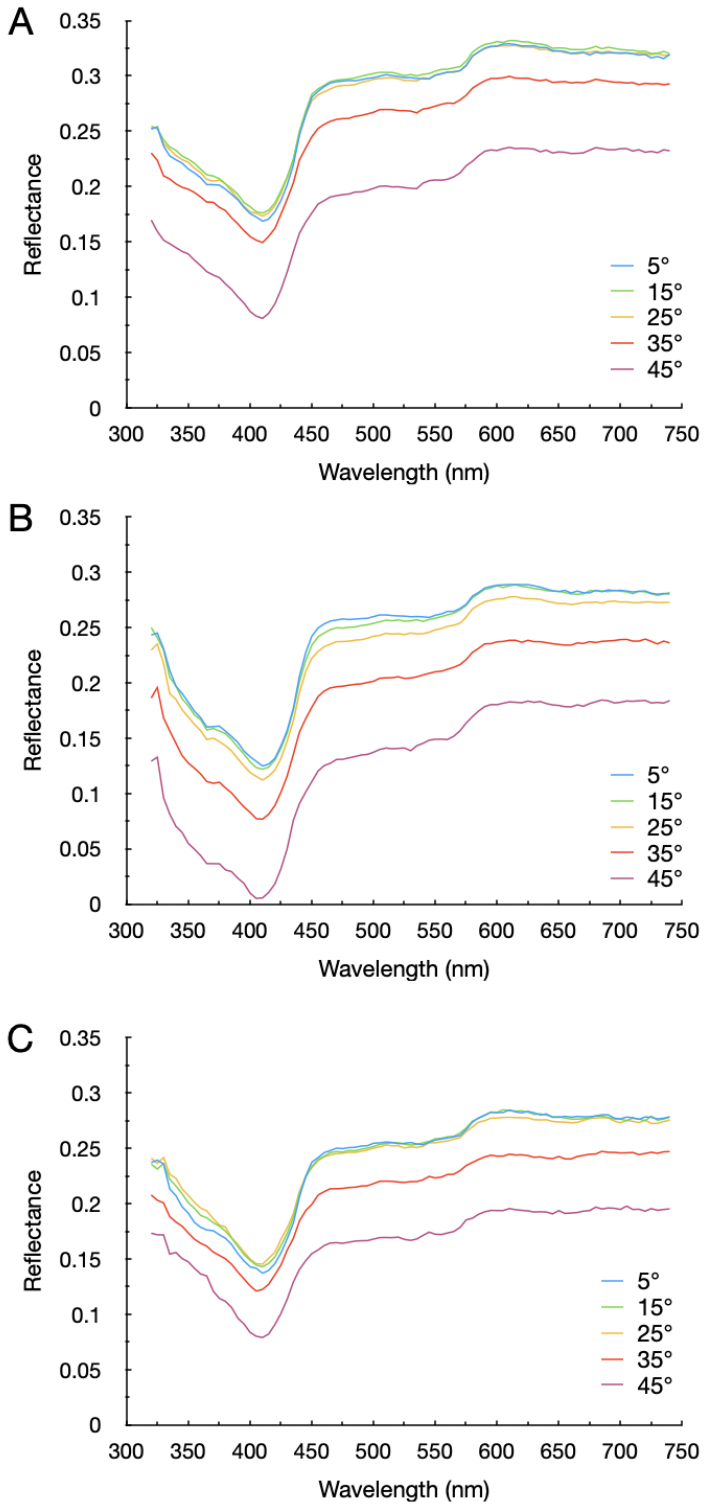

Figure 2.8 **Average relative reflectances of *Daphnia magna* (A–C) at five different angles of incidence under three different conditions of polarization: (A) unpolarized (0% polarized) light, (B) 100% P-polarized light, and (C) 100% S-polarized light.**

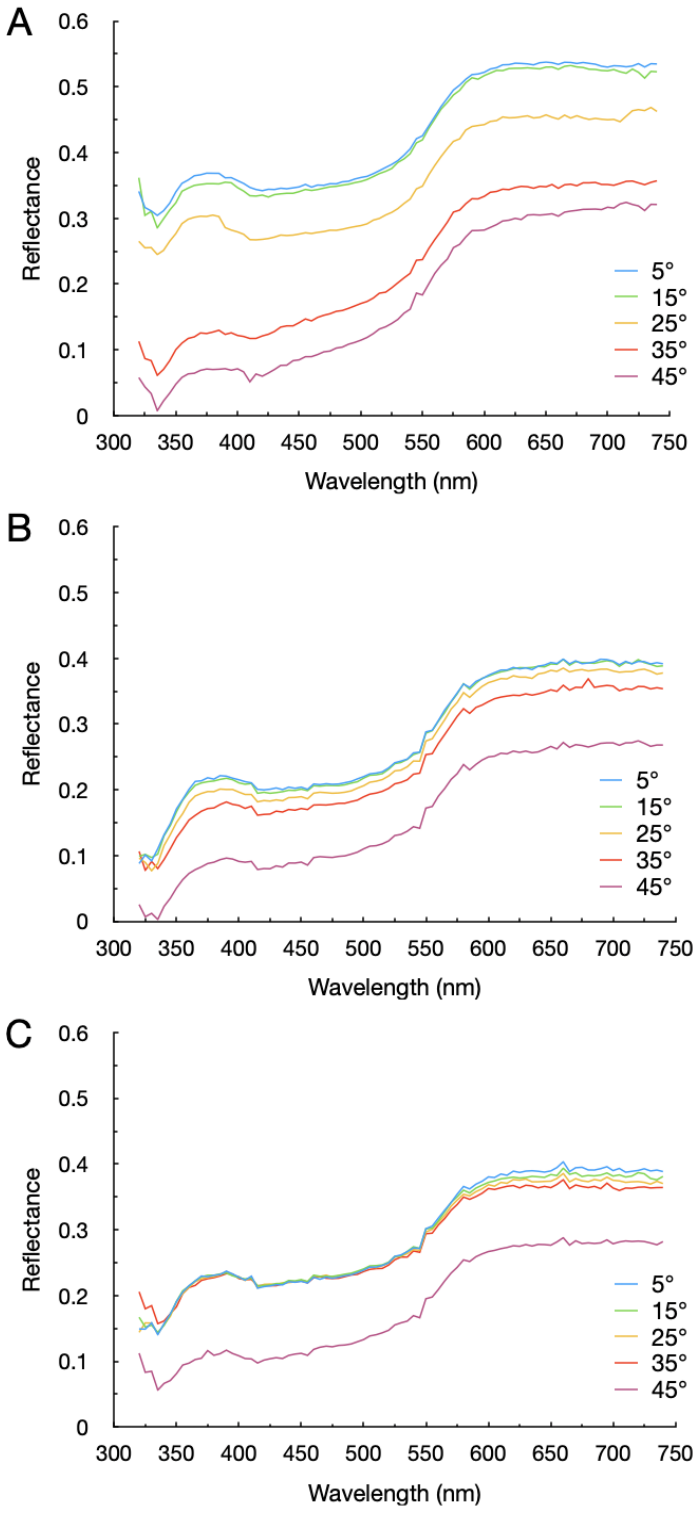

Figure 2.9 **Average relative reflectances of *Sapphirina nigromaculata* (A–C) at five different angles of incidence under three different conditions of polarization: (A) unpolarized (0% polarized) light, (B) 100% P-polarized light, and (C) 100% S-polarized light.**

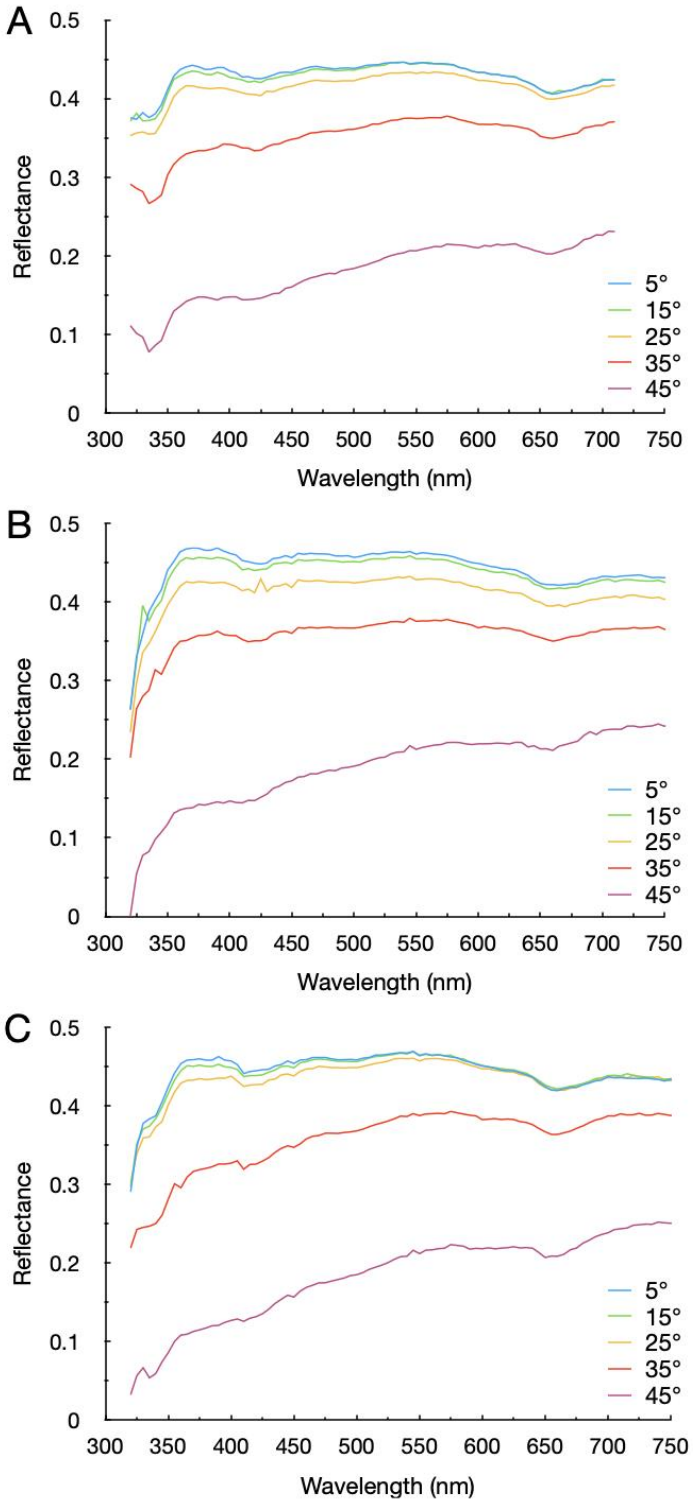

Figure 2.10 **Average relative reflectances of *Heptacarpus sitchensis* (A–C) at five different angles of incidence under three different conditions of polarization: (A) unpolarized (0% polarized) light, (B) 100% P-polarized light, and (C) 100% S-polarized light.**

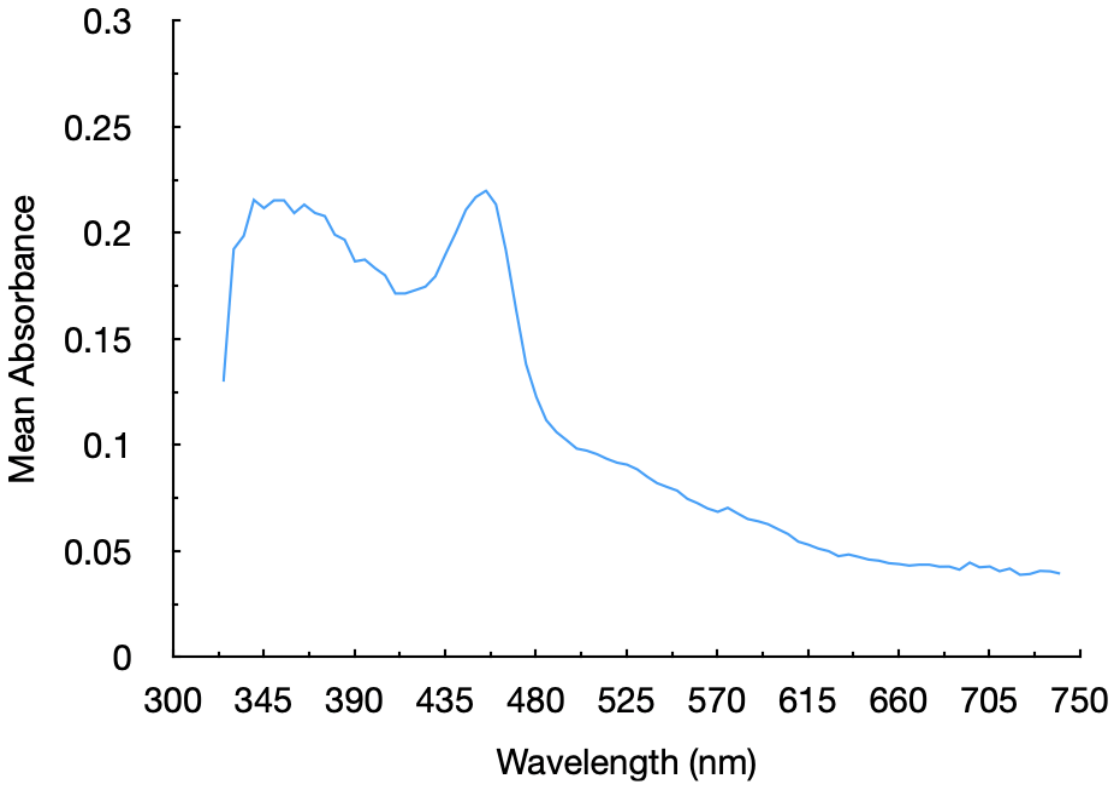

Figure 2.11 Mean absorbance of *D. magna* (n=4).

Chapter 3.

Polarization-based contrast of zooplankton

3.1. Introduction

Polarization vision is primarily a capability of invertebrate visual systems where it serves a variety of purposes including target detection, communication, and orientation (Labhart, 2016). Among vertebrates, the only species with a proven photoreceptor basis for polarization detection is the northern anchovy, *Engraulis mordax* (Novales Flamarique, 2017). Polarization discrimination in this animal arises from a set of axially dichroic photoreceptors (long and bifid cones) with an orthogonal disposition of lamellae between them. These cones alternate forming continuous rows in the ventro-temporal retina (Novales Flamarique, 2017). It has been shown that the northern anchovy uses polarization sensitivity to improve its foraging performance on zooplankton prey (Novales Flamarique, 2019).

Other fishes, such as rainbow trout (Hawryshyn and McFarland, 1987) and goldfish, *Carassius auratus* (Roberts and Needham, 2007), are believed to be polarization sensitive. However, the significance of these results has been questioned as there is no proven cellular mechanism for polarization sensitivity in other fishes besides anchovies (Novales Flamarique, 2017, 2019).

Assuming that polarization sensitivity is indeed a property of the visual systems of zebrafish and rainbow trout, this chapter explores which combination of cone interactions would be most likely to result in enhanced target contrast of zooplankton.

3.2. Methods

3.2.1. Polarization contrast of zooplankton

Polarization contrast was computed for two optical scenarios: (1) the inherent contrast of *Daphnia*, due to a potential differential reflection between P-polarized and S-polarized components by the cuticle, and (2) the contrast between *Daphnia* and the aquatic background.

The inherent contrast of *Daphnia* was calculated under two assumptions: (1) that polarization detectors are present in the retina of rainbow trout and zebrafish, and (2) that two independent detectors, maximally sensitive to P-polarized and S-polarized light, respectively, are antagonistic to each other providing the difference signal for polarization contrast.

The contrast of *Daphnia* against the background assumed that one polarization detector was maximally sensitive to S-polarized light (considered the primary reflections by *Daphnia*), whereas the other polarization detector would be tuned to P-polarized light (the primary polarization along the horizontal direction (Labhart, 2016; Johnsen et al. 2011).

In the first case, if the incident light on the *Daphnia* is unpolarized (i.e., the intensity of perpendicular polarization equals that of parallel polarization), the inherent *Daphnia* contrast can be computed as (Equation 7, see Appendix for derivation):

$$Inherent\ Contrast = \frac{|(R_S - R_P)|}{|(R_S + R_P)|} \quad (7)$$

Where R_S is the S-polarized reflectance and R_P is the P-polarized reflectance at a given wavelength.

The above equation assumes that the two retinal photoreceptors (analyzing parallel and perpendicular polarizations, respectively) have equal properties except for analyzing polarization (E-vector) direction. If this is not the case (e.g., the UV-sensitive channel being maximally sensitive to vertical polarization and the middle-wavelength sensitive channel maximally sensitive to horizontal polarization), then the absorbance properties of these photoreceptors, their neural interactions, and their relative densities need to be considered (see the Appendix). This leads to the following (Equation 8):

$$Inherent\ Contrast = \frac{|(R_S \cdot A_S \cdot cone\ ratio) - (R_P \cdot A_P)|}{|(R_S \cdot A_S \cdot cone\ ratio) + (R_P \cdot A_P)|} \quad (8)$$

Where the absorptances of the S-polarization sensitive cones are A_S, and the absorptances of the P-polarization sensitive cones are A_P (See Figure 2.7). The value of

the cone ratio depends on the frequency of the respective photoreceptor cones found in the fish retina and the number of cone types involved in the theoretical interaction.

In the second optical scenario, the contrast that arises between the *Daphnia* and the background illumination, assuming unpolarized incident light, can be formulated as (Equation 9):

$$Contrast = \frac{\left(D \cdot \frac{|(R_S - R_P)|}{|(R_S + R_P)|}\right) - (B \cdot (1 - HF))}{\left(D \cdot \frac{|(R_S - R_P)|}{|(R_S + R_P)|}\right) + (B \cdot (1 - HF))} \quad (9)$$

Where *D* is downwelling irradiance and *B* is the background sidewelling (horizontal) irradiance at a given wavelength. The horizontal factor (*HF*) is the percent of polarization of the horizontal irradiance and ranges between 10% and 70%, where the latter is the maximum percent polarization found in nature (Sabbah and Shashar, 2007).

As per the computations of inherent *Daphnia* contrast (Equation 8), if multiple photoreceptor types with different absorptance properties are involved in contrast perception, their interactions and relative densities need to be considered. The general formula then becomes:

$$Contrast = \frac{\left(D \cdot A_S \cdot cone\ ratio \cdot \frac{|(R_S - R_P)|}{|(R_S + R_P)|}\right) - (B \cdot A_P \cdot (1 - HF))}{\left(D \cdot A_S \cdot cone\ ratio \cdot \frac{|(R_S - R_P)|}{|(R_S + R_P)|}\right) + (B \cdot A_P \cdot (1 - HF))} \quad (10)$$

For both contrast scenarios (i.e., inherent to the *Daphnia* and between the *Daphnia* and the background) all potential combinations of cone mechanism interactions (i.e., UV–M, UV–L, UV– (M+L), S–M, S–L, S–(M+L), (UV+S)–(M+L), (UV–S)–(M–L), (UV+S) –M, (UV+S)–L, (UV–S)–M, (UV–S)–L) were considered for both the rainbow trout and zebrafish visual systems. This allowed a theoretical assessment of which combinations of cone photoreceptors would be most likely to enhance contrast of *Daphnia* based on polarization processing.

The contrast values derived from both Equations 8 and 10 were integrated across the spectrum (320-740 nm). The wavelength ranges of the cone absorptances (Figure 2.7) limited the contrast curves derived from Equation 8, e.g., the absorptance of

the UV-sensitive cone in rainbow trout (Figure 2.7A) is only above zero below 500 nm. Once the absorptance value approached zero, both the numerator and denominator of Equation 8 also approached zero and were erroneous, which was the reason that the resulting graphs had a limited range. The previous computations were restricted to irradiance values at 3.3 meters depth (Figure 2.5A) because percent polarization was greatest in surface waters and could accommodate the range in horizontal factor used (Novales Flamarique & Hawryshyn, 1997).

3.3. Results

3.3.1. Inherent contrasts

The inherent contrast of *Daphnia* (Figure 3.1A) was highest around 410 nm whereas that of *Sapphirina* (Figure 3.1B) peaked at 325 nm and that of *H. sitchensis* (Figure 3.1C) at 340 nm. Contrast was greater with larger angles of incidence and *H. sitchensis* had the lowest inherent contrast among all three species.

3.3.2. Inherent contrasts if photoreceptors were associated with a specific polarization-sensitive channel

The largest *Daphnia* contrasts arose for greater angles of incidence. The cone interactions resulting in the greatest contrast were (UV+S)-M (Figure 3.2) for zebrafish and (UV+S)-L (Figure 3.3) for rainbow trout. Other cone interactions also resulted in sizable inherent contrast values (Figures A2, A3, and A4). The same trends in polarization contrast were found for the other two species of zooplankton with the exception of contrasts at 45° incidence.

3.3.3. Contrasts of zooplankton against the water background

The contrasts of *Daphnia* (Figure 3.4*), Sapphirina* (Figure 3.5), and *H. sitchensis* (Figure 3.6) against the water background were positive in the shorter wavelengths (below 400 nm) and negative in the longer wavelengths for all angles of incidence. The contrasts of zooplankton against a polarized water background were more positive at higher percent polarizations, i.e., HF: 0.7 or 70%, and more negative at lower percent polarizations, i.e., HF: 0.1 or 10%. Larger percent polarization of the background resulted in more negative

contrast values. Additionally, when the background light was in the antisun direction, contrast values were generally greater than when the background light originated from the sun direction.

The range of positive contrasts for *Daphnia* was generally between 320 and 440 nm, regardless of sidewelling irradiance and angle (Figure 3.4). The range of positive contrasts for *Sapphirina* was larger—between 320 and 550 nm (Figure 3.5). Compared with the other two zooplankton species, *H. sitchensis* generally had negative contrasts (Figure 3.6). The few positive contrast values for *H. sitchensis* were mostly at high angles of incidence in the UV and red regions.

3.3.4. Contrasts of zooplankton against the water background if photoreceptors were associated with a specific polarization-sensitive channel

The (UV+S)-L cone interaction yielded the greatest contrasts for all three zooplankton species regardless of the fish visual system considered (Figure 3.7). Two additional interactions with similarly large contrasts were the (UV+S)-M and (UV-S)-L (Figures A3, A4, & A5) which also involved antagonistic interactions between short-wavelength and long-wavelength cones.

3.4. Discussion

Under backgrounds of varying percent polarization (Figure 3.7), synergetic interactions between the UV and S cones coupled to antagonism with a cone that was sensitive to longer wavelengths (either M or L) resulted in the highest theoretical contrasts for the tree species of zooplankton studied to the visual systems of both rainbow trout and zebrafish visual systems. Electrophysiological recordings have shown that shorter wavelength cone mechanisms in the retinas of rainbow trout and zebrafish are antagonistic to longer wavelength ones (Coughlin & Hawryshyn, 1994; Hughes et al., 1998), providing a physiological basis for the interactions predicted to generate high contrasts of zooplankton.

During crepuscular conditions, the ambient light shifts towards shorter wavelengths with a greater proportion of ultraviolet and short wavelength contributing to the spectrum compared to other times of the day (Novales Flamarique and Hawryshyn,

1997). In addition, the broad characteristics of the spectrum in the middle to long wavelengths (in the range ~ 480-700 nm) would make photon catch of the M and L cones similar. Thus, the contrast of zooplankton, were polarization not a factor, would likely be enhanced based on photon catch differences between shorter and longer wavelength cone mechanisms. The greatest background percent polarizations, which can reach 67% in temperate surface waters, occur at crepuscular period (Novales Flamarique and Hawryshyn, 1997). Thus, the contrasts between zooplankton and the water background (which generate primarily vertical and horizontal polarization, respectively) would be expected to increase even further for a polarization sensitive predator endowed with vertically and horizontally sensitive polarization detection channels.

It is perhaps no coincidence that foraging activity of many zooplanktivorous fishes occurs in surface waters and during crepuscular periods (Yahel et al., 2005). These are also the times when zooplankton are found near the water surface and the cone photoreceptors of fish remain active, as opposed to the rod-dominated visual system that dominates scotopic (night) conditions. The theoretical analyses presented here lend support to the evolution of visual systems with spectral or polarization sensitivities that take advantage of the crepuscular light environment and plankton ecology to enhance foraging performance.

3.5. Figures

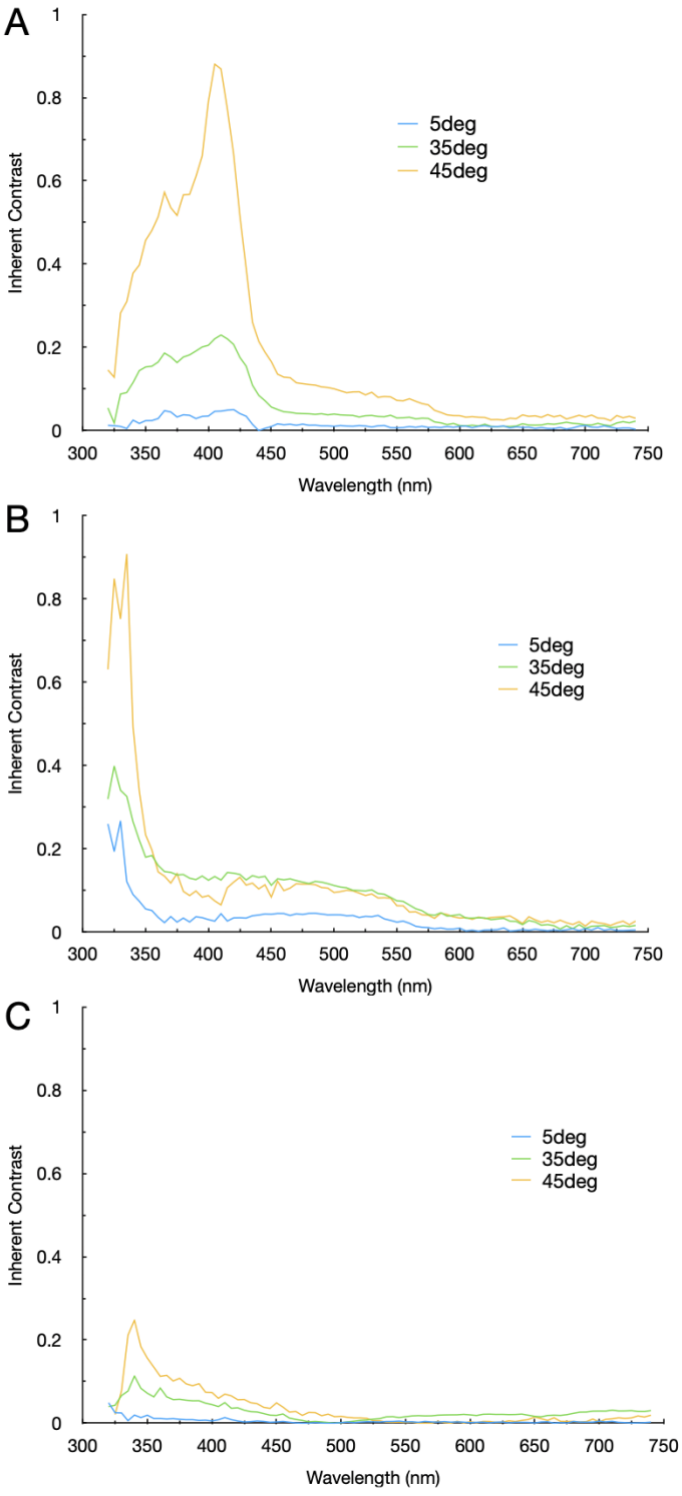

Figure 3.1 Inherent contrasts of A) *Daphnia* B) *Sapphirina* and C) *H. sitchensis*.

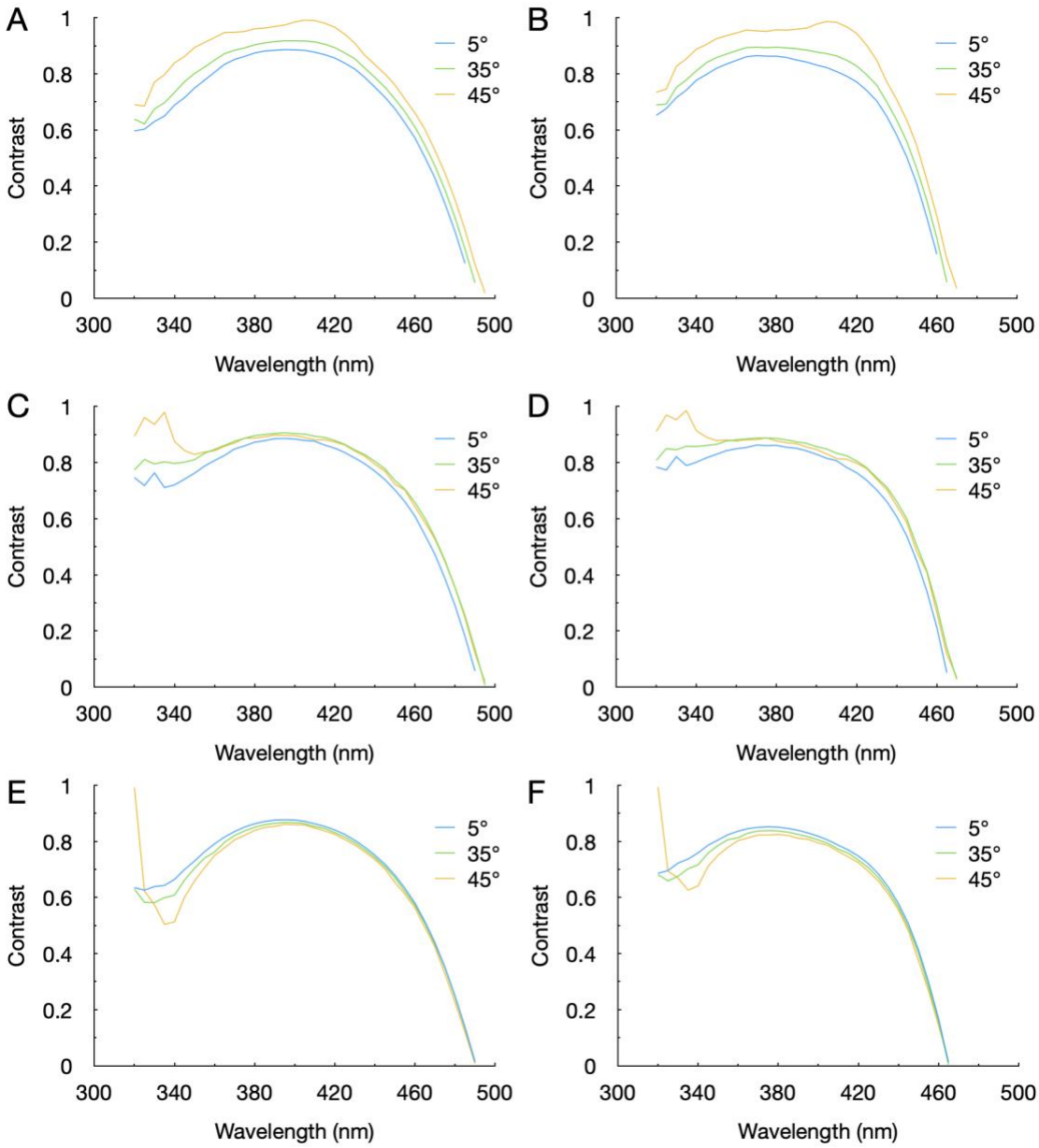

Figure 3.2 **Contrasts of *Daphnia* (A, B), *Sapphirina* (C, D), and *H. sitchensis* (E, F) when the UV and S cones are associated with P-polarization channels and the M cone with S-polarization channels (i.e., the cone interaction (UV+S)-M), based on the visual systems of rainbow trout (A, C, E) and zebrafish (B, D, F).**

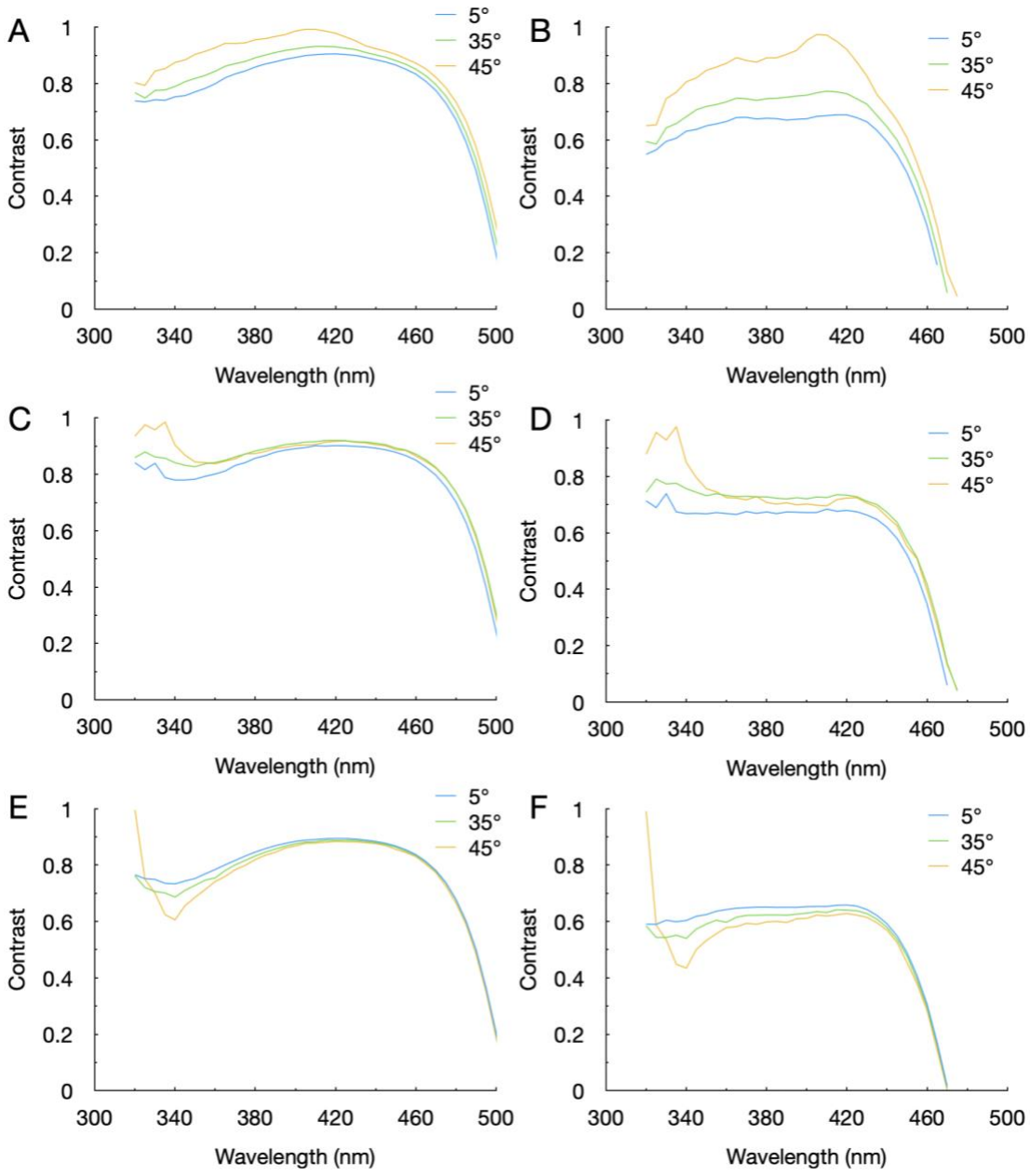

Figure 3.3 **Contrasts of *Daphnia* (A, B), *Sapphirina* (C, D), and *H. sitchensis* (E, F) when the UV and S cones are associated with P-polarization channels and the L cone with S-polarization channels (i.e., the cone interaction (UV+S)-L), based on the visual systems of rainbow trout (A, C, E) and zebrafish (B, D, F).**

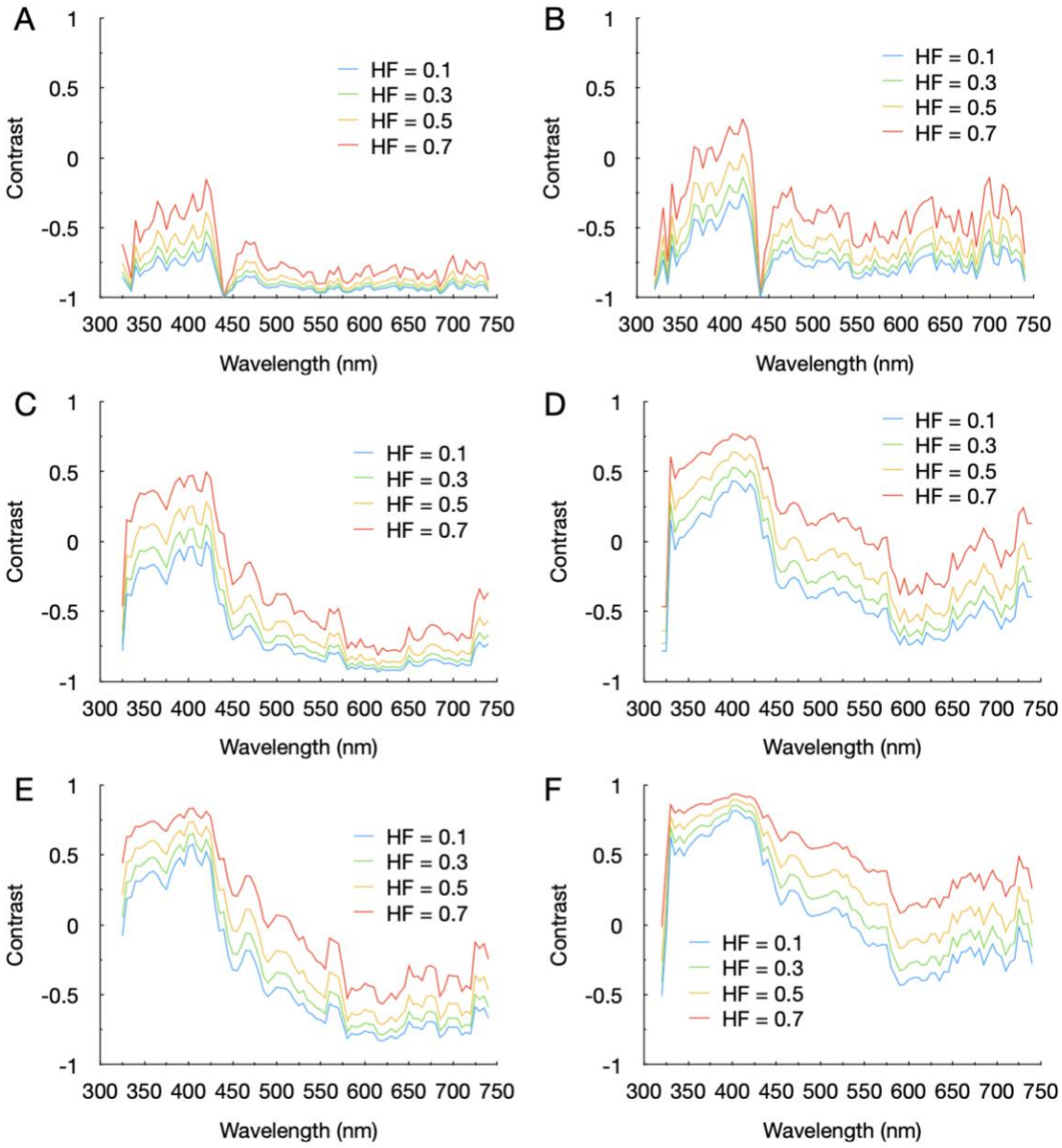

Figure 3.4 **Contrast of *Daphnia* against backgrounds of varying degrees (percent) of polarization (HF= 0.1, 0.3, 0.5, 0.7) for two orthogonal photoreceptors with identical properties except for sensitivity to the E-vector. Downwelling and sun sidewelling conditions (A, C, and E) and downwelling and antisun sidewelling conditions (B, D, F) at incident angles of 5°(A, C), 35° (C,D), and 45° (E,F).**

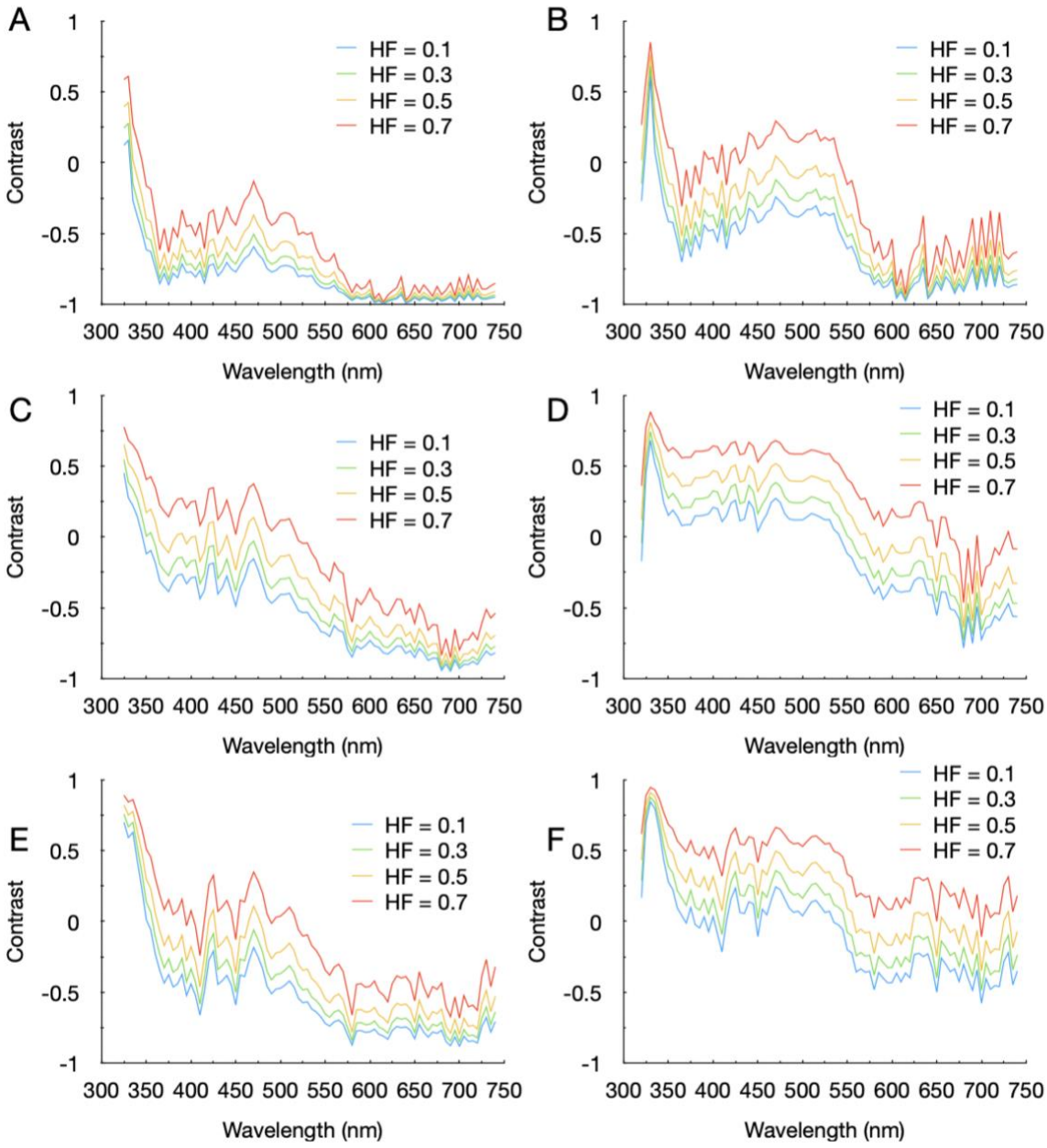

Figure 3.5 **Contrast of *Sapphirina* against backgrounds of varying degrees (percent) of polarization (HF= 0.1, 0.3, 0.5, 0.7) for two orthogonal photoreceptors with identical properties except for sensitivity to the E-vector. Downwelling and sun sidewelling conditions (A, C, and E) and downwelling and antisun sidewelling conditions (B, D, F) at incident angles of 5°(A, C), 35° (C,D), and 45° (E,F).**

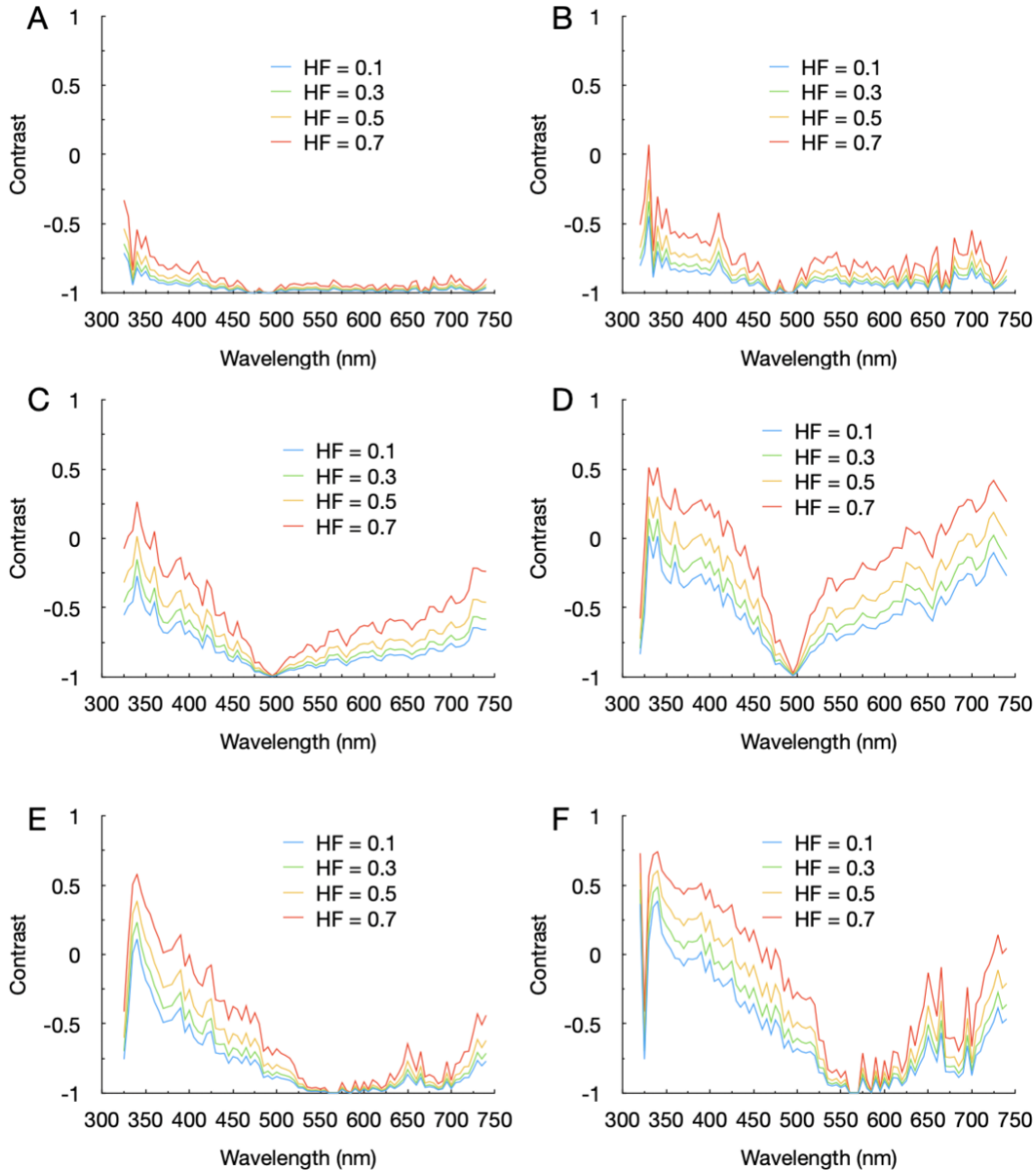

Figure 3.6 **Contrast of *H. sitchensis* against backgrounds of varying degrees (percent) of polarization (HF= 0.1, 0.3, 0.5, 0.7) for two orthogonal photoreceptors with identical properties except for sensitivity to the E-vector. Downwelling and sun sidewelling conditions (A, C, and E) and downwelling and antisun sidewelling conditions (B, D, F) at incident angles of 5°(A, C), 35° (C,D), and 45° (E,F).**

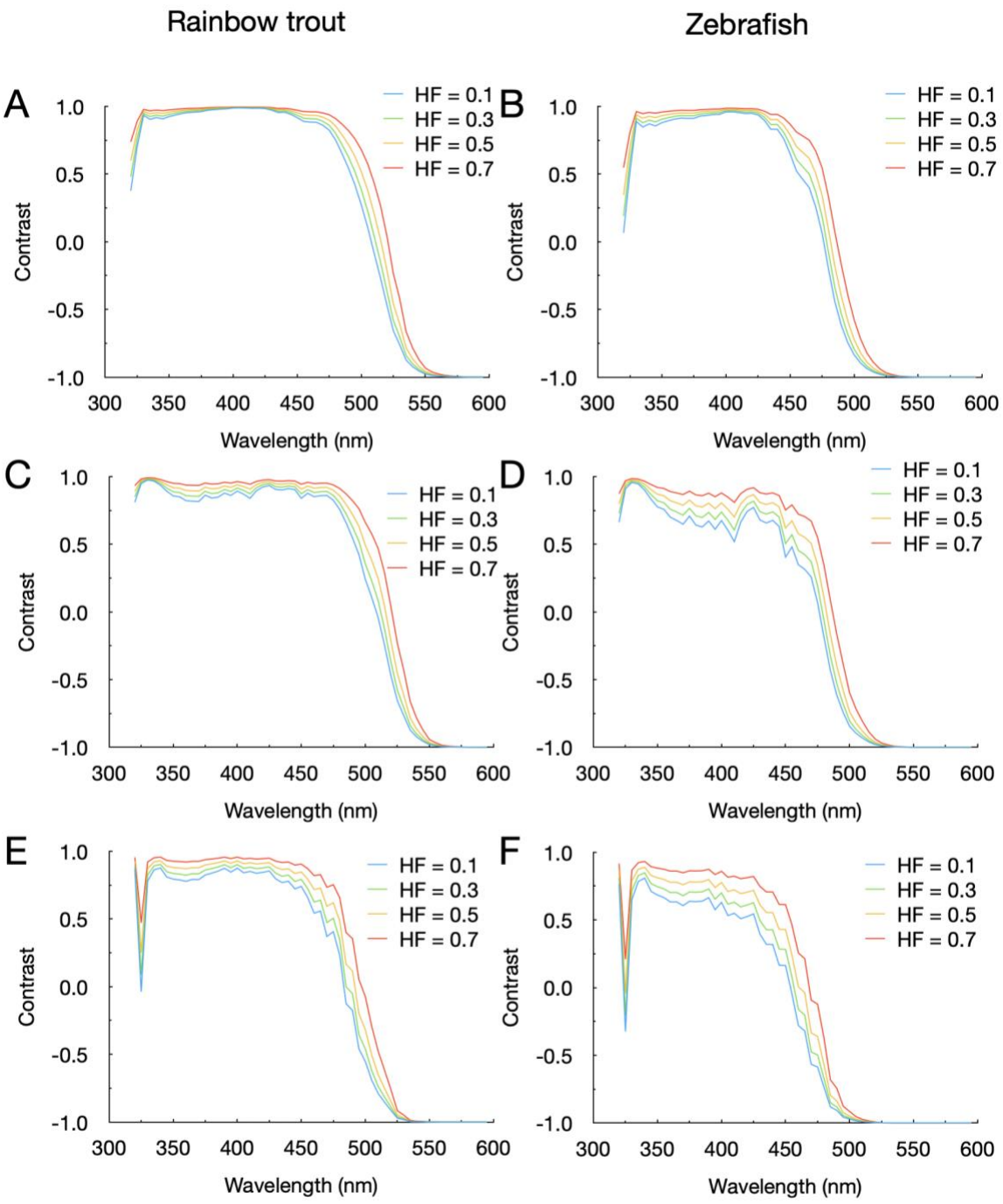

Figure 3.7 **Contrast curves for *Daphnia* (A, B), *Sapphirina* (C, D), and *H. sitchensis* (E, F) resulting from the (UV+S)-L cone interaction as a function of varying percent polarization (HF) of the background.**

Reference List

Alstad, N. E. W., Skardal, L., Hessen, D. O. (1999). The effect of calcium concentration on the calcification of *Daphnia magna*. *Limnology and Oceanography*, 44(8), 2011–2017.

Azofeifa, D. E., Arguedas, H. J., & Vargas, W. E. (2012). Optical properties of chitin and chitosan biopolymers with application to structural color analysis. *Optical Materials*, 35 (2012) 175–183.

Baar, Y., Rosen, J., & Shashar, N. (2014). Circular polarization of transmitted light by sapphirinidae copepods. *PLOS One*, 9(1), e86131.

Bagge, L. E. (2019). Not As Clear As It May Appear: Challenges Associated with Transparent Camouflage in the Ocean. *Integrative and Comparative Biology*, 59(6), 1653-1663.

BC Lake Stewardship and Monitoring Society (2014, July 9). *Cowichan Lake 2004-2013*. Retrieved October 23, 2021, from https://cowichanwatershedboard.ca/

Benoit-Bird, K. J. (2009). Dynamic 3-dimensional structure of thin zooplankton layers is impacted by foraging fish. *Marine Ecology Progress Series*, 396, 61-76.

Brierley, A. S. (2014). Diel vertical migration. *Current biology*, 24(22), R1074-R1076.

Browman, H. I., Novales Flamarique, I. & Hawryshyn, C. W. (1994). Ultraviolet photoreception contributes to prey search behaviour in two species of zooplankivorous fishes. *Journal of Experimental Biology*, 186, 187-198.

Carleton, K. L., Escobar-Camacho, D., Stieb, S. M., Cortesi, F., & Marshall, N. J. (2020). Seeing the rainbow: mechanisms underlying spectral sensitivity in teleost fishes. *Journal of Experimental Biology*, *223*(8), jeb193334.

Cheung, D. W. S., Wai, M. S. M., & Yew, D. T. (2013). The diversity of cones in the retina of vertebrates: a review. *OA Anatomy*, 1, 1-6.

Cheng, C. L., Novales Flamarique, I., Hárosi, F. I., Rickers-Haunerland, J., & Haunerland, N. H. (2006). Photoreceptor layer of salmonid fishes: transformation and loss of single cones in juvenile fish. *Journal of Comparative Neurology*, 495(2), 213-235.

Cheng, C. L., Gan, K. J., & Novales Flamarique, I. (2007). The ultraviolet opsin is the first opsin expressed during retinal development of salmonid fishes. *Investigative ophthalmology & visual science,* 48(2), 866-873.

Coughlin, D. J., & Hawryshyn, C. W. (1994). The contribution of ultraviolet and short-wavelength sensitive cone mechanisms to color vision in rainbow trout. *Brain, Behavior and Evolution*, 43(4-5), 219-232.

Cowles, D. (2014). *Heptacarpus sitchensis*. Invertebrates of the Salish Sea. https://inverts.wallawalla.edu/Arthropoda/Crustacea/Malacostraca/Eumalacostraca/Eucarida/Decapoda/Caridea/Family_Hippolytidae/Heptacarpus_sitchensis.html

Cronin, T. W. (2016). Camouflage: Being Invisible in the Open Ocean. *Current Biology*, 26, R1177–R1196.

Cronin, T. W., & Bok, M. J. (2016). Photoreception and vision in the ultraviolet. *The Journal of Experimental Biology*, 219, 2790–2801.

Cronin, T. W., & Johnsen, S. (2016). Extraocular, Non-Visual, and Simple Photoreceptors: An Introduction to the Symposium. *Integrative and Comparative Biology*, 56(5), 758–763.

Cummings, M., & Partridge, J. (2001). Visual pigments and optical habitats of surfperch (Embiotocidae) in the California kelp forest. *Journal of Comparative Physiology A*, *187*(11), 875-889.

Dalton, B. E., De Busserolles, F., Marshall, N. J., & Carleton, K. L. (2017). Retinal specialization through spatially varying cell densities and opsin coexpression in cichlid fish. *Journal of Experimental Biology*, 220(2), 266-277.

Douglas, R. H., & Jeffery, G. (2014). The spectral transmission of ocular media suggests ultraviolet sensitivity is widespread among mammals. *Proceedings of the Royal Society B,* 281, 20132995.

Ebrey, T., & Koutalos, Y. (2001). Vertebrate photoreceptors. *Progress in retinal and eye research*, 20(1), 49-94.

Fein. A. & Szuts. E.Z. (1982). *Photoreceptors: their role in vision*. Cambridge University Press.

Fineran, B. A., & Nicol, J. A. C. (1976). Novel Cones in the Retina of the Anchovy. *Journal of Ultrastructure Research*, 54, 296-303.

Fineran, B. A., & Nicol, J. A. C. (1978). Studies on the Photoreceptors of *Anchoa mitchilli* and *A. hepsetus* (*Engraulidae*) with Particular Reference to the Cones. *Philosophical Transactions of the Royal Society of London. Series B, Biological Sciences*, 283(994), 25-60.

Fratzer, C., Dörr, S. & Neumeyer, C. (1994). Wavelength Discrimination of the Goldfish in the Ultraviolet Spectral Range, *Vision Research*, 34(11), 1515–1520.

Frau, S., Novales Flamarique, I., Keeley, P. W., Reese, B. E., & Muñoz-Cueto, J. A. (2020). Straying from the flatfish retinal plan: Cone photoreceptor patterning in the common sole (*Solea solea*) and the Senegalese sole (*Solea senegalensis*). *Journal of Comparative Neurology*, 528(14), 2283-2307.

Gallager, S. M., & Mann, R. (1986). Individual variability in lipid content of bivalve larvae quantified histochemically by absorption photometry. *Journal of plankton research*, 8(5), 927-937.

Gur, D., Leshem, B., Pierantoni, M., Farstey, V., Oron, D., Weiner, S., & Addadi, L. (2015). Structural Basis for the Brilliant Colors of the Sapphirinid Copepods. *Journal of the American Chemical Society*, 137, 8408−8411.

Gur, D., Leshem, B., Farstey, V., Oron, D., Addadi, L., & Weiner, S. (2016). Light-Induced Color Change in the Sapphirinid Copepods: Tunable Photonic Crystals. *Advanced Functional Materials*, 26, 1393–1399.

Haney, J.F., et al. (2013). *An-Image-based Key to the Zooplankton of North America.* University of New Hampshire Center for Freshwater Biology. Retrieved September 16, 2021 from http://cfb.unh.edu/cfbkey/html/index.html

Hárosi, F. I. (1994). An analysis of two spectral properties of vertebrate visual pigments. *Vision research*, *34*(11), 1359-1367.

Hawryshyn, C. W., & McFarland, W. N. (1987). Cone photoreceptor mechanisms and the detection of polarized light in fish. *Journal of Comparative Physiology A*, 160, 459-465.

Hays, G. C. (2003). A review of the adaptive significance and ecosystem consequences of zooplankton diel vertical migrations. *Migrations and dispersal of marine organisms*, 163-170.

Hecht, E., & Zajac, A. (1987). *Optics*. Addison-Wesley.

Hessen, D. O., Alstad, N. E. W., & Skardal, L. (2000). Calcium limitation in *Daphnia magna. Journal of Plankton Research*, 22(3), 553–568.

Hoke, K. L., Evans, B. I., & Fernald, R. D. (2006). Remodeling of the cone photoreceptor mosaic during metamorphosis of flounder (*Pseudopleuronectes americanus*). *Brain, behavior and evolution*, 68(4), 241-254.

Hughes, A., Saszik, S., Bilotta, J., DeMarco, P., & Patterson, W. (1998). Cone contributions to the photopic spectral sensitivity of the zebrafish ERG. *Visual Neuroscience, 15*(6), 1029-1037.

Jacobs, G. H. (1992). Ultraviolet vision in vertebrates. *American Zoologist*, *32*(4), 544-554.

Johnsen, S., Marshall, N. J., & Widder, E. A. (2011). Polarization sensitivity as a contrast enhancer in pelagic predators: lessons from in situ polarization imaging of transparent zooplankton. *Philosophical Transactions of the Royal Society B: Biological Sciences*, *366*(1565), 655-670.

Kennedy, D., & Milkman, R. D. (1956). Selective light absorption by the lenses of lower vertebrates, and its influence on spectral sensitivity. *The Biological Bulletin* 111(3), 375-386.

Kondrashev, S. L., Gnyubkina, V. P., & Zueva, L. V. (2012). Structure and spectral sensitivity of photoreceptors of two anchovy species: *Engraulis japonicus* and *Engraulis encrasicolus*. *Vision Research*, 68, 19–27.

Kondrashev, S., Kornienko, M., Gnyubkina, V. & Frolova, L. (2016). Intraretinal variability and specialization of cones in Japanese anchovy (*Engraulis japonicus*, Engraulidae). *Journal of Morphology*, 277: 472-481.

Labhart, T. (2016). Can invertebrates see the e-vector of polarization as a separate modality of light? *Journal of Experimental Biology*, 219 (24): 3844–3856.

Lampert, W. (1989). The adaptive significance of diel vertical migration of zooplankton. *Functional ecology*, 21-27.

Land, M. F. (1966). A multilayer interface reflector in the eye of the scallop, *Pecten maximus*. *The Journal of Experimental Biology*, 45, 433-447.

Levine, J. S. (1985). The vertebrate eye. In *Functional Vertebrate Morphology*. (pp. 317-337). Harvard University Press. https://doi.org/10.4159/harvard.9780674184404.c16

Levine, J. S., & MacNichol, E. F. (1982). Color vision in fishes. *Scientific American*, 246(2), 140-149.

Loew, E. R., McFarland, W. N., Mills, E. L., & Hunter, D. (1993). A chromatic action spectrum for planktonic predation by juvenile yellow perch, *Perca flavescens. Canadian Journal of Zoology*. 71: 384-386.

Lvovsky, A. I. (2013). Fresnel Equations. *Encyclopedia of Optical Engineering*. (pp. 1-6) Taylor and Francis, New York.

Marshall, N. J., Cortesi, F., de Busserolles, F., Siebeck, U. E., & Cheney, K. L. (2019). Colours and colour vision in reef fishes: Past, present and future research directions. *Journal of Fish Biology*, 95(1), 5-38.

Neville, A.C. (1975). Physical Properties. In *Biology of the Arthropod Cuticle*. Zoophysiology and Ecology, vol 4/5. Springer, Berlin, Heidelberg.

Novales Flamarique, I. (2013). Opsin switch reveals function of the ultraviolet cone in fish foraging. *Proceedings of the Royal Society B*, 280, 20122490.

Novales Flamarique, I. (2016). Diminished foraging performance of a mutant zebrafish with reduced population of ultraviolet cones. *Proceedings of the Royal Society B*, 283, 20160058.

Novales Flamarique, I. (2017). A vertebrate retina with segregated colour and polarization sensitivity. *Proceedings of the Royal Society B*, 284, 20170759.

Novales Flamarique, I. (2019). Swimming behaviour tunes fish polarization vision to double prey sighting distance. *Scientific Reports*, 9(1), 1–8.

Novales Flamarique, I. & Browman, H. (2001). Foraging and prey-search behaviour of small juvenile rainbow trout (*Oncorhynchus mykiss*) under polarized light. *The Journal of Experimental Biology*, 204, 2415-2422.

Novales Flamarique, I., & Hárosi, F. I. (2002). Visual pigments and dichroism of anchovy cones: A model system for polarization detection. *Visual Neuroscience*, 19, 467–473.

Novales Flamarique, I. & Wachowiak, M. (2015). Functional segregation of retinal ganglion cell projections to the optic tectum of rainbow trout. *Journal of Neurophysiology,* 114: 2703–2717.

Novales Flamarique, I., Hendry, A., & Hawryshyn, C. W. (1992). The Photic Environment of a Salmonid Nursery Lake. *Journal of Experimental Biology*, 169(1), 121-141.

Otte, K. A., Fröhlich, T., Arnold, G. J., & Laforsch, C. (2014). Proteomic analysis of *Daphnia magna* hints at molecular pathways involved in defensive plastic responses. *BMC genomics*, 15(1), 1-17.

Ouseph, P. J., Driver, K., & Conklin, J. (2001). Polarization of light by reflection and the Brewster angle. *American Journal of Physics*, 69, 1166-1168.

Razouls C., Desreumaux N., Kouwenberg J. & de Bovée F. (2021). Biodiversity of Marine Planktonic Copepods (morphology, geographical distribution and biological data). Sorbonne University, CNRS. Retrieved April 28, 2021, from http://copepodes.obs-banyuls.fr/en

Raymond, P. A., Colvin, S. M., Jabeen, Z., Nagashima, M., Barthel, L. K., Hadidjojo, J., Popova, L., Pejaver, V. R., & Lubensky, D. K. (2014). Patterning the cone mosaic array in zebrafish retina requires specification of ultraviolet-sensitive cones. *PLOS One*, 9(1), e85325.

Rick, I. P., Bloemker, D., & Bakker, T. C. M. (2012). Spectral composition and visual foraging in the three-spined stickleback (Gasterosteidae: *Gasterosteus aculeatus* L.): elucidating the role of ultraviolet wavelengths. *Biological Journal of the Linnean Society*, 105 (2), 359–368.

Risner, M. L., Lemerise, E., Vukmanic, E. V., & Moore, A. (2006). Behavioral spectral sensitivity of the zebrafish (*Danio rerio*). *Vision research*, *46*(17), 2625-2635.

Roberts, N. W., & Needham, M. G. (2007). A mechanism of polarized light sensitivity in cone photoreceptors of the goldfish *Carassius auratus*. *Biophysical Journal*, 93(9), 3241-3248.

Sabbah, S., & Shashar, N. (2007). Light polarization under water near sunrise. *JOSA A*, *24*(7), 2049-2056.

Savelli, I., & Novales Flamarique, I. (2018). Variation in opsin transcript expression explains intraretinal differences in spectral sensitivity of the northern anchovy. *Visual neuroscience*, 35.

Savelli, I., Novales Flamarique, I., Iwanicki, T., & Taylor, J. S. (2018). Parallel opsin switches in multiple cone types of the starry flounder retina: tuning visual pigment composition for a demersal life style. *Scientific reports*, 8(1), 1-10.

Schurcliff, W. A. (1962). *Polarized light: production and use*. Harvard University Press.

Siebeck, U. E., Parker, A. N., Sprenger, D., Mäthger, L. M., & Wallis, G. (2010). A species of reef fish that uses ultraviolet patterns for covert face recognition. *Current Biology*, 20, 407 – 410.

Silberglied, R. E. (1979). Communication in the ultraviolet. *Annual Review of Ecology and Systematics*, 10(1), 373-398.

Shashar, N., Hanlon, R. T., & Petz, A. D. (1998). Polarization vision helps detect transparent prey. *Nature*, 393(6682), 222-223.

Taylor, J. L. (2013). *Integrating Sphere Functionality: The Scatter Transmission Measurement.* PerkinElmer. https://resources.perkinelmer.com/corporate/cmsresources/images/44-156124tch_011486_01_integratingspherefunctionalitythescattertransmissionmeasurement.pdf

Titelman, J., Varpe, Ø., Eliassen, S., & Fiksen, Ø. (2007). Copepod mating: chance or choice?. *Journal of Plankton Research*, 29(12), 1023-1030.

Yahel, R., Yahel, G., Berman, T., Jaffe, J. S., & Genin, A. (2005). Diel pattern with abrupt crepuscular changes of zooplankton over a coral reef. *Limnology and Oceanography*, 50(3), 930-944.

Yokoyama, S. (2000). Molecular evolution of vertebrate visual pigments. *Progress in retinal and eye research*, 19(4), 385-419.

Yoshimatsu, T., Schröder, C., Nevala, N. E., Berens, P., and Baden, T. (2020). Fovea-like Photoreceptor Specializations Underlie Single UV Cone Driven Prey-Capture Behavior in Zebrafish. *Neuron*, 107, 320–337.

Zimmermann, M. J. Y., Nevala, N. E., Yoshimatsu, T., Osorio, D., Nilsson, D., Berens, P. & Baden, T. (2018). Zebrafish Differentially Process Color across Visual Space to Match Natural Scenes. *Current Biology*, 28(13), 2018-2031.e6.

Zukoshi R., Savelli, I., & Novales Flamarique, I. (2018). Foraging performance of two fishes, the threespine stickleback and the Cumaná guppy, under different light backgrounds. *Vision Research*, 145, 31-38.

Appendix. Supplemental Information

Figures

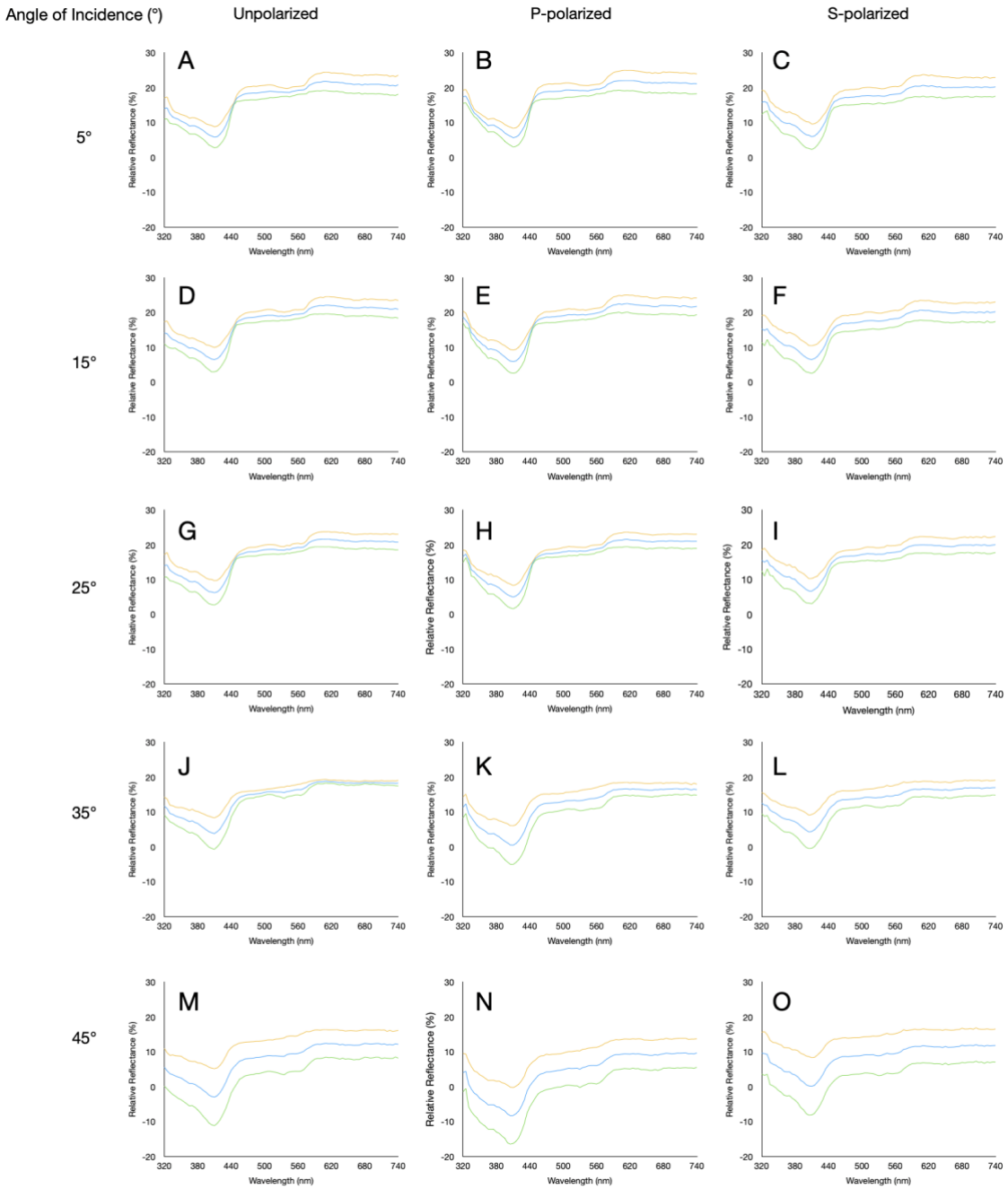

Figure A1 **Mean reflectance (± SE) for *Daphnia* illuminated by unpolarized (A, D, G, J, M), P-polarized (B, E, H, K, N), and S-polarized (C, F, I, L, O) light at five different angles of incidence. The blue function is the mean reflectance, whereas the yellow and green functions are the upper and lower SE limits, respectively.**

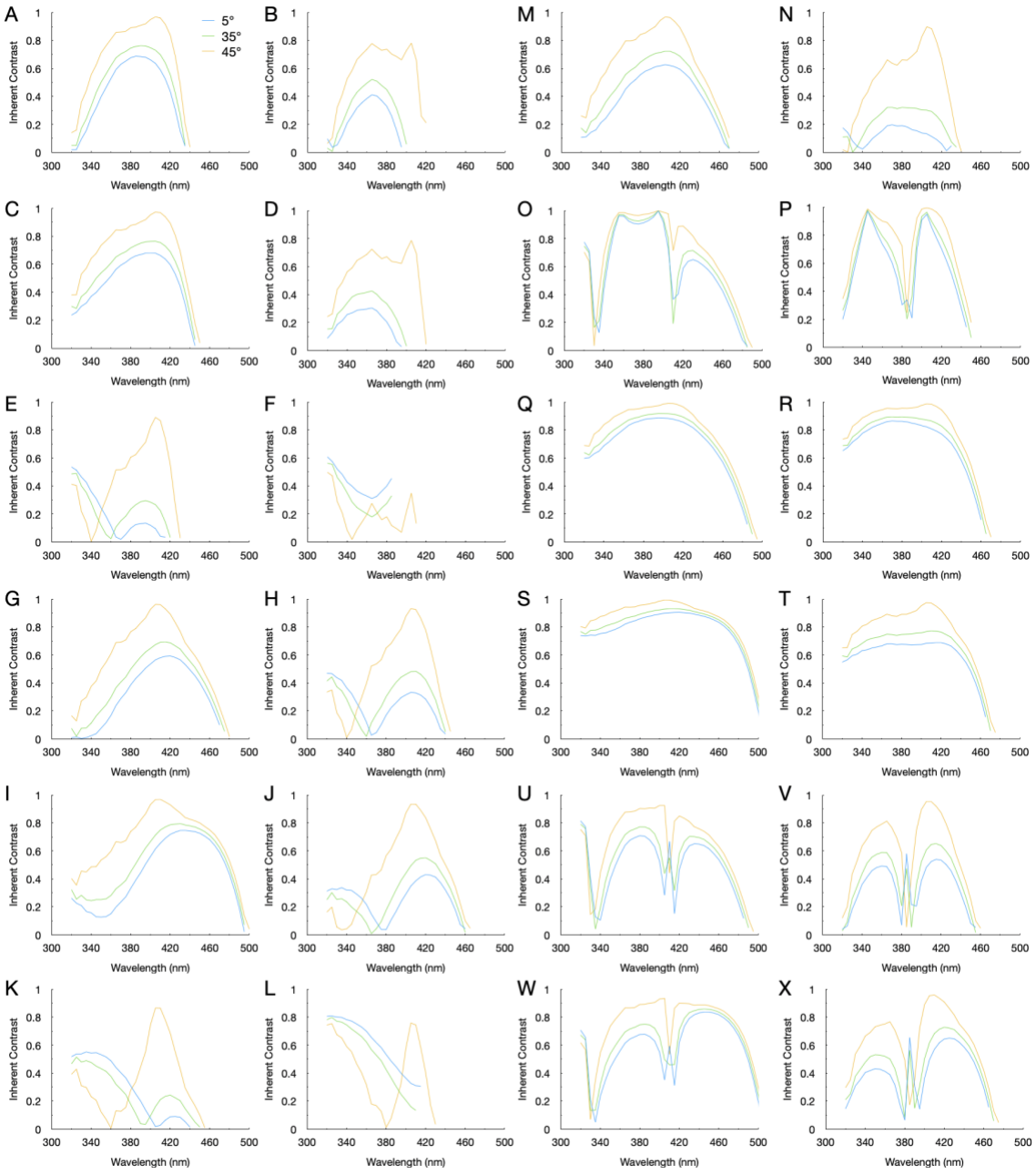

Figure A2 **Predicted inherent contrast of *Daphnia* using visual system parameters for rainbow trout (A, C, E, G, I, K, M, O, Q, S, U, and W) and zebrafish (B, D, F, H, J, L, N, P, R, T V, X). The cone interactions modeled were as follows: UV–M (A, B), UV–L (C, D), UV–(M+L) (E, F), B–M (G, H), B–L (I, J), B–(M+L) (K, L), (UV+S)–(M+L) (M, N), (UV–B)–(M–L) (O, P), (UV+S)–M (Q, R), (UV+S)–L (S, T), (UV–B)–M (U, V), and (UV–B)–L (W, X).**

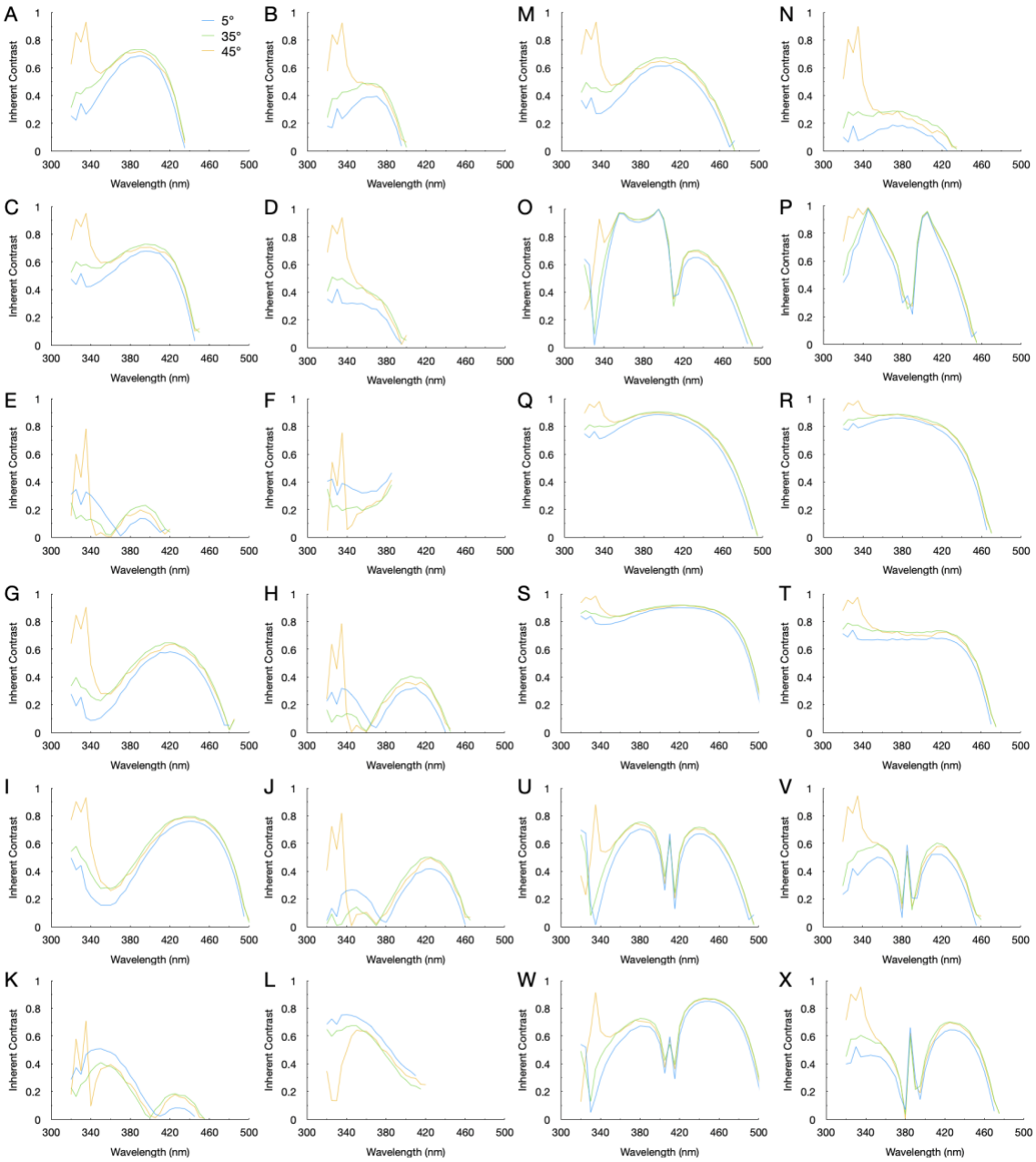

Figure A3 **Predicted inherent contrast of *Sapphirina nigromaculata* using visual system parameters for rainbow trout (A, C, E, G, I, K, M, O, Q, S, U, and W) and zebrafish (B, D, F, H, J, L, N, P, R, T V, X). The cone interactions modeled were as follows: UV–M (A, B), UV–L (C, D), UV–(M+L) (E, F), B–M (G, H), B–L (I, J), B–(M+L) (K, L), (UV+S)–(M+L) (M, N), (UV–B)–(M–L) (O, P), (UV+S)–M (Q, R), (UV+S)–L (S, T), (UV–B)–M (U, V), and (UV–B)–L (W, X).**

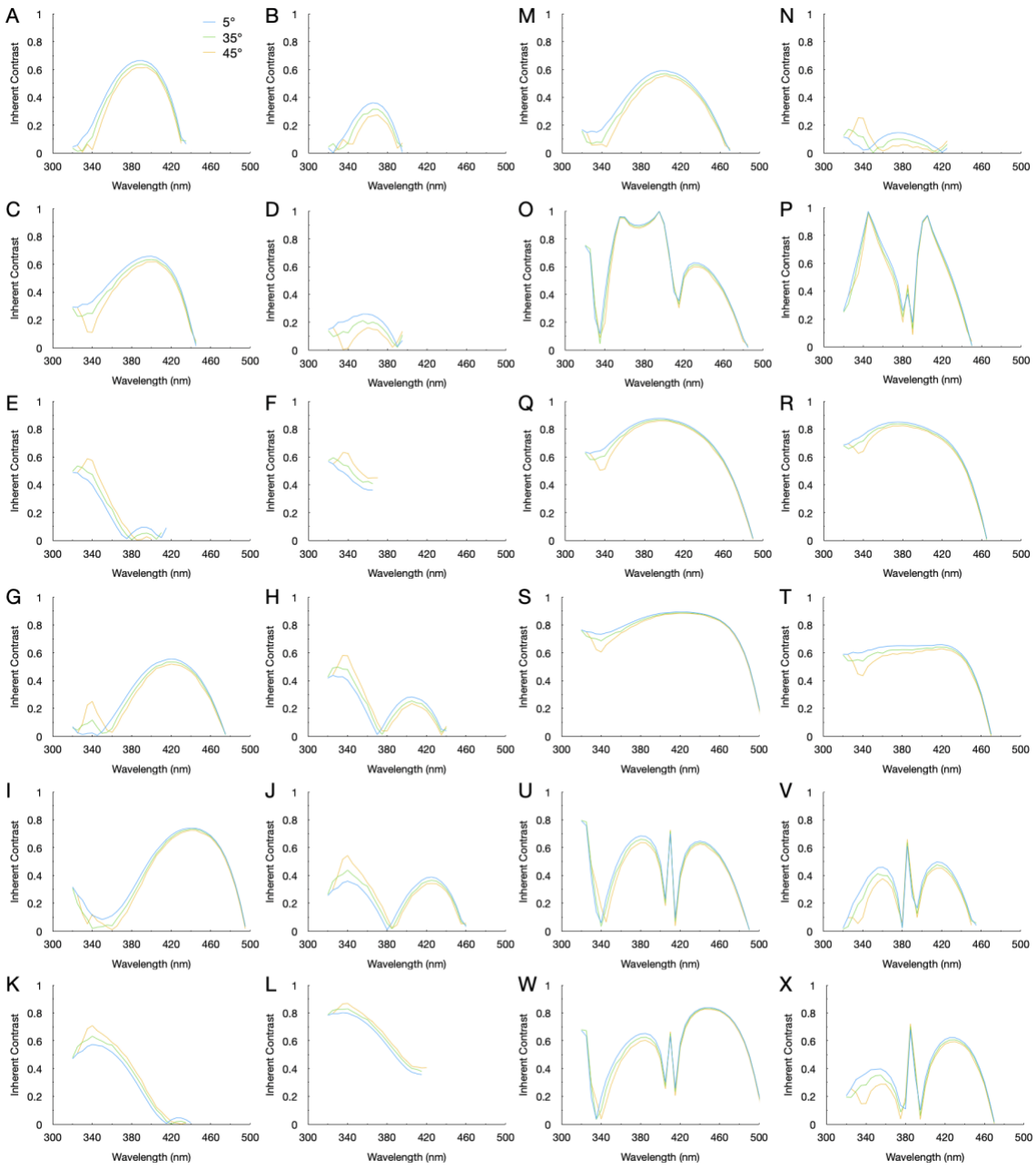

Figure A4 **Predicted inherent contrast of *Heptacarpus sitchensis* using visual system parameters for rainbow trout (A, C, E, G, I, K, M, O, Q, S, U, and W) and zebrafish (B, D, F, H, J, L, N, P, R, T V, X). The cone interactions modeled were as follows: UV–M (A, B), UV–L (C, D), UV–(M+L) (E, F), B–M (G, H), B–L (I, J), B–(M+L) (K, L), (UV+S)–(M+L) (M, N), (UV–B)–(M–L) (O, P), (UV+S)–M (Q, R), (UV+S)–L (S, T), (UV–B)–M (U, V), and (UV–B)–L (W, X).**

Chapter 3 Equations to Model Zooplankton Contrast

Two cases were considered in order to estimate the contrast of zooplankton. The first case determined the inherent contrast of the zooplankton (contrast due to reflections from within the zooplankton) as perceived by the parallel (P) and perpendicular (S) polarization channels of the fish's visual system.

In the first case, contrast would be generally defined as:

$$Contrast = \frac{|(Daphnia_S - Daphnia_P)|}{|(Daphnia_S + Daphnia_P)|} \quad \text{(A1)}$$

Where $Daphnia_s$ is the quantum catch of the photoreceptor processing the perpendicular reflectance and $Daphnia_p$ is the quantum catch of the photoreceptor processing the parallel reflectance.

Thus, the $Daphnia_s$ and $Daphnia_p$ components are:

$$Daphnia_S = \frac{D \cdot P_S \cdot R_S}{(R_S + R_P)} \quad \text{(A2)}$$

$$Daphnia_P = \frac{D \cdot P_P \cdot R_P}{(R_S + R_P)} \quad \text{(A3)}$$

Where D is the downwelling irradiance, P_S and P_P are the fractions of downwelling irradiance with E-vector either in the perpendicular and parallel directions, respectively. R_S and R_P are the reflectances of the *Daphnia* in the perpendicular and parallel directions, respectively.

If P_S is equal to P_P, the inherent contrast of *Daphnia* (Equation A1) by integrating Equations A2 and A3 would be:

$$Contrast = \frac{|(R_S - R_P)|}{|(R_S + R_P)|} \quad \text{(A4)}$$

To only determine the difference between the reflected polarization components, the absolute values were included. This scenario assumed that the two photoreceptors (for sensing P-polarized and S-polarized light) have equal properties, except for sensitivity to an E-vector.

If certain photoreceptors were associated with specific polarization channels, then the photon catches for both *Daphnia*$_s$ and *Daphnia*$_p$ needed to be included to account for the properties of the associated photoreceptors:

$$Daphnia_S = \left[\frac{D \cdot P_S \cdot R_S}{(R_S + R_P)}\right] \cdot A_S \cdot (cone\ ratio) \quad \text{(A5)}$$

$$Daphnia_P = \left[\frac{D \cdot P_P \cdot R_P}{(R_S + R_P)}\right] \cdot A_P \quad \text{(A6)}$$

Where A_S was the combined absorptance of photoreceptors associated with the S-polarization channel, and A_P was the absorptance of photoreceptors associated with the P-polarization channel. The *cone ratio* was the proportion of specific types of photoreceptors (i.e., UV, S, M, or L) in a given fish species. All four cone types were equal in quantity in rainbow trout, but in zebrafish, there were two M or L cones for every one UV or S cone.

If P_S is equal to P_P, the inherent contrast of *Daphnia* (Equation A1) with Equations A5 and A6 could be simplified to:

$$Contrast = \frac{|(R_S \cdot A_S \cdot cone\ ratio) - (R_P \cdot A_P)|}{|(R_S \cdot A_S \cdot cone\ ratio) + (R_P \cdot A_P)|} \quad \text{(A7)}$$

The following cone interactions were computing using Equation A7, wherein the first cone(s) corresponded to the S-polarized reflected components and the second cone(s) corresponded to the P-polarized background components: UV-M, UV-L, UV-(M+L), S-M, S-L, S-(M+L), (UV+S)-(M+L), (UV-S)-(M-L), (UV+S)-M, (UV+S)-L, (UV-S)-M, and (UV-S)-L.

The second case determined the contrast of *Daphnia* against the water background:

$$Contrast = \frac{\left|(P_{Daphnia} - P_{Background})\right|}{\left|(P_{Daphnia} + P_{Background})\right|} \quad \text{(A8)}$$

Where $P_{Daphnia}$ is the component of light reflected by the *Daphnia* and $P_{background}$ is the component of background irradiance. We assume that there are two polarization channels, with one sensitive to S-polarized reflections of the downwelling from *Daphnia* and the other to P-polarized light from the water background. We also assume that the downwelling irradiance on the *Daphnia* is unpolarized. Thus, polarization contrast from the *Daphnia* solely arises from the difference in reflectance and absorbance of the two polarization components, i.e., S and P.

The proportion of S-polarized light reflected from the *Daphnia* and absorbed by the S-polarization sensitive photoreceptor would be:

$$P_{Daphnia} = D \cdot Pol_S \cdot \frac{|(R_S - R_P)|}{|(R_S + R_P)|} \quad \text{(A9)}$$

And the proportion of P-polarized light from the background would be:

$$P_{Background} = B \cdot Pol_P \cdot (1 - HF) \quad \text{(A10)}$$

Where Pol_S and Pol_P represented various properties of the photoreceptor, e.g., absorptance. *B* represented the background sidewelling irradiance, and *HF* (horizontal factor) was the percentage of P-polarization from the background sidewelling irradiance**.**

If Pol_S is equal to Pol_P, contrast becomes:

$$Contrast = \frac{\left(D \cdot Pol_S \cdot \frac{|(R_S - R_P)|}{|(R_S + R_P)|}\right) - (B \cdot Pol_P \cdot (1 - HF))}{\left(D \cdot Pol_S \cdot \frac{|(R_S - R_P)|}{|(R_S + R_P)|}\right) + (B \cdot Pol_P \cdot (1 - HF))} \quad \text{(A11)}$$

If Pol_S does not equal Pol_P, then:

$$Contrast = \frac{\left(D \cdot \frac{|(R_S - R_P)|}{|(R_S + R_P)|}\right) - (B \cdot (1 - HF))}{\left(D \cdot \frac{|(R_S - R_P)|}{|(R_S + R_P)|}\right) + (B \cdot (1 - HF))} \quad \text{(A12)}$$

We assume that the two photoreceptors (for analyzing S and P polarizations) have equal properties except for their sensitivity to the E-vector.

Similar to Equation A7, if certain photoreceptors are only associated with specific polarization channels, then the photon catch components would need to take into account the various photoreceptors associated with each polarization-sensitive channel and their interactions. Contrast in this case would then be:

$$Contrast = \frac{\left(D \cdot A_S \cdot cone\ ratio \cdot \frac{|(R_S - R_P)|}{|(R_S + R_P)|}\right) - (B \cdot A_P \cdot (1 - HF))}{\left(D \cdot A_S \cdot cone\ ratio \cdot \frac{|(R_S - R_P)|}{|(R_S + R_P)|}\right) + (B \cdot A_P \cdot (1 - HF))} \quad \text{(A13)}$$

Similar to the first case, we then looked at the following cone interactions for the above equation, wherein the first cone(s) correspond to the reflected component (A_S) and the second cone(s) correspond to the background component (A_P): UV-M, UV-L, UV-(M+L), S-M, S-L, S-(M+L), (UV+S)-(M+L), (UV-S)-(M-L), (UV+S)-M, (UV+S)-L, (UV-S)-M, and (UV-S)-L.